URT
AND
16 NOVEMBER 1979 (FOUO 4/79) 1 OF 1

JPRS L/8768

16 November 1979

# USSR Report

## PHYSICS AND MATHEMATICS

(FOUO 4/79)

FBIS FOREIGN BROADCAST INFORMATION SERVICE

NOTE

JPRS publications contain information primarily from foreign newspapers, periodicals and books, but also from news agency transmissions and broadcasts. Materials from foreign-language sources are translated; those from English-language sources are transcribed or reprinted, with the original phrasing and other characteristics retained.

Headlines, editorial reports, and material enclosed in brackets [] are supplied by JPRS. Processing indicators such as [Text] or [Excerpt] in the first line of each item, or following the last line of a brief, indicate how the original information was processed. Where no processing indicator is given, the information was summarized or extracted.

Unfamiliar names rendered phonetically or transliterated are enclosed in parentheses. Words or names preceded by a question mark and enclosed in parentheses were not clear in the original but have been supplied as appropriate in context. Other unattributed parenthetical notes within the body of an item originate with the source. Times within items are as given by source.

The contents of this publication in no way represent the policies, views or attitudes of the U.S. Government.

For further information on report content call (703) 351-2938 (economic); 3468 (political, sociological, military); 2726 (life sciences); 2725 (physical sciences).

JPRS L/8768

16 November 1979

# USSR REPORT

## PHYSICS AND MATHEMATICS

(FOUO 4/79)

This serial publication contains articles, abstracts of articles and news items from USSR scientific and technical journals on the specific subjects reflected in the table of contents.

Photoreproductions of foreign-language sources may be obtained from the Photoduplication Service, Library of Congress, Washington, D.C. 20540. Requests should provide adequate identification both as to the source and the individual article(s) desired.

CONTENTS PAGE

CONTENTS (Continued) Page

ACOUSTICS

UDC 534+534.231.2

# ARRIVAL ANGLE FLUCTUATIONS OF A PLANE WAVE PROPAGATING IN A SEA MEDIUM AS RECEIVED BY A LINEAR ARRAY

Moscow AKUSTICHESKIY ZHURNAL in Russian Vol 25, No 4, 1979 pp 625-628

[Article by V. A. Yeliseyevnin, Acoustics Institute USSR Academy of Sciences, submitted for publication 26 July 1978, after revision 11 January 1979]

[Text] Sound propagation in a sea medium is accompanied by its scattering on random volumetric inhomogeneities of the water layer, and also on bottom irregularities and the wave-covered sea surface, which leads, in particular, to fluctuations of the angle of arrival of a wave at the antenna. Similar fluctuations are investigated in [1-3] applicable to the scattering of optical and radio waves in a turbulent atmosphere or ionosphere. Fluctuations of the direction of a sound ray, reflected from an uneven sea surface, are considered in [4], but the computations are made without taking the size of the receiver aperture into account.

Below we compute the dispersions of fluctuations of the angle of arrival of a plane wave at a linear array, the wave being multiply reflected from the wave-covered sea surface, and also scattered on turbulent inhomogeneities of the water layer.

According to [1], the angle of wave arrival on the antenna will be considered as the angular coordinate of the "center of gravity" of the displaced image $\alpha_0$, which applicable to the considered case of a linear antenna can be written in the form

$$\alpha_0 = \frac{\int_{-\infty}^{+\infty} \alpha I(\alpha)\, d\alpha}{\int_{-\infty}^{+\infty} I(\alpha)\, d\alpha} = \frac{1}{jk} \frac{\int_{-L/2}^{+L/2} \Psi_0(\eta)\, d\Psi_0^*(\eta)}{\int_{-L/2}^{+L/2} |\Psi_0(\eta)|^2\, d\eta}, \qquad (1)$$

where $\Psi_0(\eta)$ is the stipulated random distribution of the field in the antenna aperture, $I(\alpha)$ is the distribution of image intensity with respect to the $\alpha$ angle, L is the extent of the linear antenna, k is the wave number, j is a fictitious unit, * is the complex conjugation symbol.

Neglecting fluctuations of amplitude and limiting ourselves to an examination only of random phase delays, that is, representing the field in the aperture in the form $\Psi_0(\eta) = \exp[-jS(\eta)]$, where $S(\eta)$ is the random phase distribution, expression (1) can be reduced to the form

$$\alpha_0 = (1/kL)[S(L/2) - S(-L/2)]. \quad (2)$$

The dispersion of fluctuation of the arrival angle will be

$$\sigma_\alpha^2 = \overline{\langle\alpha_0^2\rangle} = (2/k^2L^2)[B_S(0) - B_S(L)] = D_S(L)/k^2L^2, \quad (3)$$

where $B_S(L)$ and $D_S(L)$ are the correlation and structural phase functions in the antenna aperture; the " — " symbol denotes averaging for a set of records.

Now we will determine the dispersion of fluctuations of the angle of arrival of a plane wave at a linear antenna, the wave being multiply reflected from the wave-covered sea surface. The problem is solved in the following formulation. Assume that a plane wave is propagated in a water layer with a constant speed of sound in the layer, a smooth rigid bottom and a wave-covered water-air surface, successively being reflected from the bottom and surface. The uneven water-air discontinuity is homogeneous, an isotropic, on the average horizontal surface $z = \zeta(x, y)(\langle\zeta(x, y)\rangle = 0)$ with unevennesses distributed in accordance with the normal law. The latter are characterized by the mean square value $\sigma_\zeta = \sqrt{\langle\zeta^2(x,y)\rangle}$ and the spatial correlation coefficient $\Gamma_\zeta(\rho) = \exp[-(\rho/a_\zeta)^2]$, where $a_\zeta$ is the correlation radius of the unevennesses and $\rho = \sqrt{x^2 + y^2}$.

Reception is accomplished on a linear antenna with a constant response along the entire length L (in the computations assigned the value unity), situated in the vertical or horizontal plane normal to the ray, experiencing mirror reflection from the mean boundary of the uneven surface.

The sound field, multiply scattered by the wave-covered sea surface, can be computed by the Kirchhoff method in an Ekrat approximation in accordance with a scheme reducing multiple reflections to single reflections, multiply repeated [5]. It is assumed that the unevennesses of the surface are so gently sloping that their slopes can be neglected and only the displacement of the surface from the mean plane need be taken into account.

By analogy with the case of single touching of an uneven surface by a ray [6], in the case of n-fold tangency the random phase delay can be written in the form

$$S(x, y) = -j2k \sin\psi \sum_{i=1}^{n} \zeta_i(x, y), \quad (4)$$

where $\psi$ is the glancing angle of the ray at the point of mirror reflection, $\zeta_L$ is the surface rise at the point of t-fold ray tangency. Assuming that the correlation radius of the unevennesses $a_\zeta$ is much less than the distance between the adjacent points of tangency of the uneven surface by the ray, the correlation function of phase fluctuations in the antenna aperture can be represented in the form

$$B_S(\eta-\eta')=4k^2 \sin^2 \psi n \sigma_\zeta^2 \Gamma_\zeta(\eta-\eta'). \quad (5)$$

Substituting this expression into formula (3) and taking into account that in the case of an antenna situated in the vertical plane the projection of $a_\zeta$ onto the antenna is equal to $a_\zeta \sin \psi$, and in the case of an antenna situated in the horizontal plane is equal to the value $a_\zeta$ itself, we obtain the following expressions for the dispersions of fluctuations of the angles of arrival of a plane wave at an antenna situated in the vertical plane

$$\sigma_{\alpha B}^2 = \frac{8n \sin^2 \psi \sigma_\zeta^2}{L^2}\left[1-\exp\left(-\frac{L^2}{a_\zeta^2 \sin^2 \psi}\right)\right] \quad (6)$$

[B = vertical] and at any antenna situated in the horizontal plane:

$$\sigma_{\alpha r}^2 = \frac{8n \sin^2 \psi \sigma_\zeta^2}{L^2}\left[1-\exp\left(-\frac{L^2}{a_\zeta^2}\right)\right]. \quad (7)$$

It can be seen from the latter two expressions that the fluctuations of the angle of wave arrival at the antenna increase with an increase in the number of reflections n, the dispersion of fluctuations of the unevennesses $\sigma_\zeta^2$ and the glancing angle of the ray $\psi$ with tangency on an uneven surface. On the other hand, the fluctuations decrease with an increase in the dimensions of the antenna L (averaging effect of the aperture) and the correlation radius of surface unevennesses $a_\zeta$. Thus, in the case of small glancing angles $\psi$ antennas of large dimensions L will not "sense" fluctuations of the angles of arrival -- a rough surface becomes a mirror surface for them.

For convenience in computations expressions (6) and (7) can be combined into one:

$$\sigma_\alpha^2=8n\tilde{\sigma}^2[1-\exp(-\tilde{L}^2)], \quad (8)$$

where the generalized parameters are $\tilde{\sigma} = \sigma_\zeta \sin \psi/L$, and $\tilde{L} = L/a_\zeta \sin \psi$, when the antenna is situated in the vertical plane, and $L = L/a_\zeta$, when the antenna is situated in the horizontal plane.

Figure 1 shows the dependences of the mean square angle of arrival of a plane wave at the antenna $\sigma_\alpha$ (in degrees) in dependence on the generalized parameters $\tilde{L}$ and $\tilde{\sigma}$ for a single reflection from an uneven surface n = 1. For n-fold reflection from an uneven surface similar dependences can be obtained by multiplying the values presented in Fig. 1 by the $\sqrt{n}$ value. The values of the generalized parameters for which the computations were made were selected proceeding on the basis of data on sea waves cited in [7].

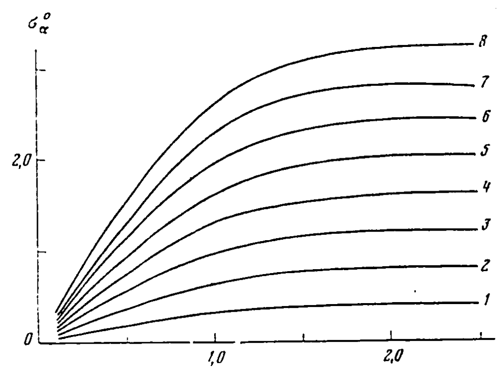


Fig. 1. Values of the mean square angle of arrival of a plane wave at a linear antenna, the wave being singly reflected from the wave-covered sea surface. The curves 1-8 correspond to the values of the generalized parameter $\sigma$ = 0.0025, 0.005,...,0.02.

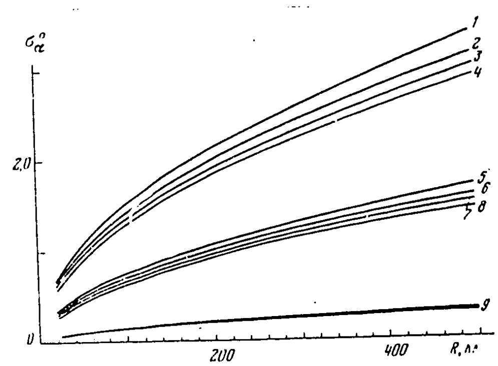


Fig. 2. Values of mean square angle of arrival of a plane wave at a linear antenna, the wave having passed through a layer of a turbulent medium of the thickness R. The curves 1-4 correspond to the values L = 10, 15, 20 and 25 m and $C_n = 10^{-4}$ $m^{-1/3}$; the curves 5-8 -- L = 10, 15, 20 and 25 m and $C_n = 5\cdot10^{-5}$ $m^{-1/3}$; curve 9 -- L = 10, 15, 20 and 25 m and $C_n = 10^{-5}$ $m^{-1/3}$.

Now we will determine the dispersion of fluctuations of the angle of arrival of a plane wave at a linear antenna, the wave being propagated in a turbulent sea medium. In [1], in the first approximation of the smooth perturbations method, the author determined the structural function of phase fluctuations of a plane wave passing through a layer of an isotropic turbulent medium of the thickness R:

$$D_S(L)=2{,}91\varkappa C_n^2 k^2 R L^{5/3}, \qquad (9)$$

where k = 0.5 when $L \leqslant \sqrt{\lambda R}$ and k = 1 when $L \geqslant \sqrt{\lambda R}$, $\lambda$ is wavelength, $C_n$ is the structural constant of the refractive index of the sea medium. [It is demonstrated in [8] that the values of the phase fluctuations obtained by this method are also correct where it is inadmissible, that is, in the region of strong fluctuations of amplitude or at very great distances.] Substituting expression (9) into formula (3), we obtain an expression for the dispersion of fluctuations of the angle of arrival of a plane wave at a linear antenna, the wave having passed through the layer of a turbulent medium:

$$\sigma_\alpha^2 = 2.91\, \kappa C_n^2 R L^{-1/3}. \qquad (10)$$

Figure 2 shows the dependence of the mean square angle of arrival of a plane wave at an antenna $\sigma_\alpha$ (in degrees), computed using the last formula, on the distance R for antennas with an aperture 10, 15, 20 and 25 m. The computations were made for values of the structural constant $C_n = 10^{-4}$, $5 \cdot 10^{-5}$ $m^{-1/3}$, characteristic for regions of the world ocean with a stable hydrological picture [7].

In conclusion it must be noted that both in the case of scattering on an uneven sea surface and in the case of scattering on three-dimensional inhomogeneities of the sea medium the computations of fluctuations of the angles of wave arrival at the antenna were made without taking into account acoustic refraction in the water layer. Computations of the field scattered by an uneven sea surface were made for the simplest model of the mechanism of scattering. Finally, it was assumed that only one ray, experiencing scattering, is incident on the antenna. These circumstances, simplifying the real situation, must be taken into account in a comparison of the results of computations and experimental data.

BIBLIOGRAPHY

1. Tatarskiy, V. I., RASPROSTRANENIYE VOLN V TURBULENTNOY ATMOSFERE (Wave Propagation in a Turbulent Atmosphere), Moscow, "Nauka," Chapter 4, 1967.

2. Shifrin, Ya. S., VOPROSY STATISTICHESKOY TEORII ANTENN (Problems in the Statistical Theory of Antennas), Moscow, "Sovetskoye Radio," 1970.

3. Lobkova, L. M., STATISTICHESKAYA TEORIYA ANTENN SVERKHVYSOKIKH I OPTICHESKIKH CHASTOT (Statistical Theory of Superhigh and Optical Frequency Antennas), Moscow, "Svyaz'," 1975.

4. Frolov, V. M., "Fluctuations of Direction of a Ray Reflected from a Statistically Uneven Surface," VOPROSY SUDOSTROYENIYA, SERIYA AKUSTIKA (Problems in Shipbuilding, Acoustics Series), 8, 74-79, 1977.

5. Gulin, E. P., "Correlation Properties of a Sound Wave With Multiple Reflections from an Uneven Surface," AKUST. ZH. (Acoustics Journal, 22, 6, 845-857, 1976.

6. Bass, F. G., Fuks, I. M., RASSEYANIYE VOLN NA STATISTICHESKI NEROVNOY POVERKHNOSTI (Wave Scattering on a Statistically Uneven Surface), Moscow, "Nauka," 1972.

7. AKUSTIKA OKEANA (Ocean Acoustics), edited by L. M. Brekhovskikh, Moscow, "Nauka," Chapter 1, 1974.

8. Klyatskin, V. I., "Dispersion of the Angle of Arrival of a Plane Light Wave Propagating in a Medium With Weak Random Inhomogeneities," IZV. VUZov, RADIOFIZIKA (News of Institutions of Higher Education, Radiophysics), 12, 5, 723-726, 1969.




5303
CSO: 8144/1928

ELECTRICITY AND MAGNETISM

UDC621.378.33

# THE DYNAMIC CHARACTERISTICS OF A FAST-FLOW ELECTRIC DISCHARGE $CO_2$ LASER

Moscow KVANTOVAYA ELEKTRONIKA in Russian Vol 6 No 7, Jul 1979 signed to press 25 Nov 78 pp 1554-1556

[Article by V. A. Artamonov and A. P. Napartovich]

[Text] The dynamic characteristics of a fast-flow electric discharge continuous $CO_2$ laser were investigated. It is shown that turbulent fluctuations in the flow of the active medium affect the laser generation dynamics along with cavity vibration and current source fluctuations.

Investigation of the factors influencing the laser emission dynamics is of decisive significance for developing dynamic control systems of laser emission parameters. It is known that emission fluctuations have technical reasons and are determined mainly by cavity vibrations and noise of the pumping source in continuous sealed-off $CO_2$ lasers [1]. It was found in measurements of the time emission characteristics of a steady fast-flow electric discharge laser (BEL) that the emission is fluctuating in nature [2, 3].

The given paper is devoted to investigating the causes of emission fluctuations of BEL with transverse pumping, operating on a mixture of atmospheric air and $CO_2$, excited by a self-sustained direct current discharge. A similar description of the experimental installation and its parameters is given in [4]. The flow of the active medium in the BEL is usually turbulent. The Reynolds number $Re \approx 10^4$ significantly exceeds the critical value of $Re_0 = 2 \cdot 10^3$ in the experimental installation. A stable cavity configuration was used whose optical axis was either combined with the lower flow boundary of the discharge zone (a "combined cavity"; in this case the discharge was excited in an air-$CO_2$ mixture) or was located at a distance of 15-20 mm down the flow from the $CO_2$ mixing collector to the vibrationally-excited air flow ("dispersed cavity").

The cavity was formed by two opaque spherical mirrors and the emission was released by means of a planoparallel plate of KCl, installed between the mirrors at an angle of 45° to the optical axis. In this case, the transverse modes were selected by using diaphragms installed in front of one of the cavity mirrors. The cavity was arranged on a vibration-insulated suspension in a vacuum chamber adjacent to the channel of the flow-through part of the laser. The cavity configuration was selected as stable to avoid development of autooscillation of the generation mode, inherent to fast-flow lasers with unstable cavities [5].

The output power was measured, the emission field distribution in the transverse section of the beam was recorded and oscillograms of the variable component of discharge flow, output power and relative percentage modulation were photographed in the experiments. The frequency spectrum of discharge current fluctuations and output power was analyzed by using a spectral analyzer of type S4-12. Moreover, the dependence of the amplification factor on the optical axis of the cavity on pumping current was measured prior to measuring the characteristics of output emission, which made it possible to link the observed emission characteristics to the excess above the generation threshold in processing the results. The output power was measured by using standard devices of type IMO-2, IOMP or calorimeters, the emission fluctuations were recorded by using a cooled photoresistor of type FSG-223, while current fluctuations were measured by a resistance shunt. The transverse emission field distribution was recorded on thermally activated photographic paper [6].

Taking oscillographs of the BEL emission showed that random modulation of emission, the depth of which varies over a wide range, is almost always observed in practice. Typical oscillograms of the integral emission and discharge current fluctuations are presented in Figure 1.

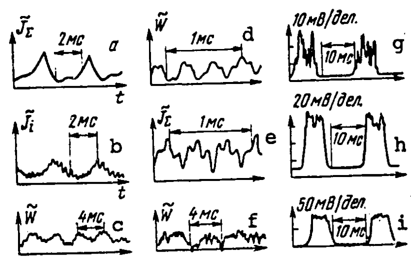


Figure 1.

To explain the effect of fast transverse pumping of the active medium on the dynamic characteristics of emission, comparative measurement of the emission characteristics were made in an ordinary tubular $CO_2$ laser with weak pumping of the medium, excited by a longitudinal DC electric discharge, along the optical axis of the cavity (Re $\approx$ 10). The oscillograms of emissivity $\tilde{W}$ and of discharge current $\tilde{I}_{\Sigma}$ during operation of the laser in the main transverse mode and at a single spectral line are presented in Figure 1, d and e, for this case. The similarity of the oscillograms and the identity of the emission fluctuation and discharge current spectra indicate that the emission fluctuations observed in this case are related mainly to current instability. The relative instability of output power does not exceed approximately 1 percent at current instability of approximately 2 percent.

An oscillogram of the variable component of BEL discharge current is presented in Figure 1, a. Fluctuations at frequency of 300 Hz are determined by the electrical circuit of the power supply source. The relative amplitude of these fluctuations comprises approximately 2 percent. Fluctuations of the kilohertz band are easily discernible on the oscillogram of the variable component of current on an individual electrode $\tilde{I}_i$ (Figure 1, b) besides fluctuations at frequency of 300 Hz. The reason for these fluctuations is apparently local random oscillations in the gas discharge plasma, caused by turbulent gas-dynamic fluctuations which are described in [7]. The fact that no kilohertz fluctuations are observed in the complete current spectrum may be explained by the absence of correlation of turbulent fluctuations through the volume of the laser discharge chamber. The oscillogram of the emission fluctuations of a BEL with combined cavity (Figure 1, c) is similar to the current oscillogram on an individual electrode (Figure 1, b). The fluctuation spectra are similar to each other and attenuate with an increase of frequency. The similarity of the current and emission fluctuation spectra indicates the weak influence of averaging along the optical axis and the absence of averaging during motion of the resulting inhomogeneity through the discharge. The observed frequencies of kilohertz emission fluctuations permit one to estimate the typical correlation dimension of inhomogeneity L in the flow: $L \approx (v/\nu - l)$, where $\nu$ is the typical fluctuation frequency, v is the flow velocity and l is the dimension of the transverse mode in the cavity. This formula was found on the assumption that the emission fluctuations occur upon intersection of the generation zone by moving inhomogeneity. For a combined cavity under typical experimental conditions, $L \approx$ 10-17 mm.

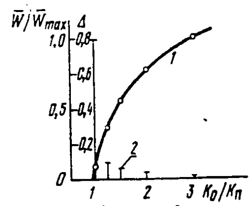

Figure 2.

Measurements of the relative percentage modulation of the output power $\Delta_W = |W_m - W|/W$ ($W_m$ is the maximum or minimum and W is the mean value of emissive power) showed that $\Delta_W$ decreases with an increase of pumping in the given emission mode. Oscillograms are presented in Figure 1, g-i and the dependence of output emissivity (1) and $\Delta_W$ (2) in the main transverse mode on the value of $\varkappa = K_0/K_p$, where $K_0$ is the weak signal amplification factor and $K_p$ is the threshold value of the amplification factor on the optical axis of the cavity ($\varkappa$ = 1.25, 2.5 and 4.3, respectively, in Figure 1, g-i), is presented in Figure 2. The functions observed in Figure 2 are explained by the nonlinear interaction of the inverse medium with the emission field inside the cavity. Actually, if the expression for output power from [8] is simplified by disregarding the relaxation processes on the transverse mode dimension, we find $W = \alpha v(1 + X_N/X_C)F$, where $\alpha$ is the numerical coefficient, $X_C$ and $X_N$ are the partial volumetric $CO_2$ and $N_2$

concentrations, while function F satisfies the equation $F = \varkappa\ (1 - e^{-F})$. From the expression for output power, it is easy to find

$$\Delta w = \Delta_v + \Delta_{xC} \pm \Delta_\varkappa (1 - \varkappa e^{-F})^{-1}.$$

For $\varkappa \gg 1\ \Delta w = \Delta_v + \Delta_{xC} + \Delta_\varkappa$, and near the generation threshold it is described by a hyperbolic function: $\Delta w = \Delta_\varkappa / (\varkappa - 1)$. Comparison of the emission fluctuations of combined (see Figure 1, c) and dispersed (Figure 1, f) cavities shows that the fluctuations are higher frequency with completely identical configuration in a dispersed cavity, which is apparently related to the turbulizing effect of the $CO_2$ mixing collector. Analysis of the typical dimension of turbulence yields in this case L = 3-6 mm, i.e., a value similar to the dimensions of the tubes of the mixing collector.

Conversion to generation in higher-order transverse modes having large volume leads to a decrease of $\Delta w$, which is apparently related to averaging of perturbations through the field volume inside the cavity.

Thus, the volume of the generating mode must be increased and one must work in the significant excess mode on generation threshold ($\varkappa \gtrsim 3$) where linear dependence of the emission fluctuations on perturbations is observed, to increase the emission stability of a steady BEL, besides vibrational insulation of the cavity design. A further increase of stability can be achieved by increasing the stability of the power supply source, improving the flow parameters of the medium and the pumping homogeneity in the BEL channel.

BIBLIOGRAPHY


1. Abdumalikov, A. Kh. et al, in: "III Respublikanskaya konferentsiya molodykh fizikov AN UzSSR" [Third Republic Conference of Young Physicists of the Uzbek SSR Academy of Sciences], Tashkent FAN, 1976.

2. Artamonov, A. V. and V. G. Naumov, KVANTOVAYA ELEKTRONIKA, Vol 4, 1977.

3. Yodev, M. J. and D. R. Ahouse, APPL. PHYS. LETTS., Vol 27, 1975.

4. Artamonov, A. V., A. A. Vedenov, A. F. Vitshas and V. G. Naumov, KVANTOVAYA ELEKTRONIKA, Vol 4, 1977.

5. Dreyzin, Yu. A. and A. M. Dykhne, PIS'MA V ZhETF, Vol 19, 1974.

6. Advertisement of State Optical Institute imeni S. I. Vavilov, KVANTOVAYA ELEKTRONIKA, Vol 5, 1978.

7. Akishev, Yu. S. and A. P. Napartovich, FIZIKA PLASMY, Vol 4, 1978.

8. Vedenov, A. A. and A. P. Napartovich, TVT, Vol 12, 1974.


[156-652]]



6521
CSO: 1862

ELECTRICITY AND MAGNETISM

UDC621.378.324

INVESTIGATING THE ACTIVE MEDIUM OF A FAST-FLOW $CO_2$ LASER WITH NON-SELF-SUSTAINED DISCHARGE

Moscow KVANTOVAYA ELEKTRONIKA in Russian Vol 6 No 7, Jul 1979 signed to press 9 Oct 78 pp 1442-1445

[Article by A. V. Artamonov, V. G. Naumov, L. V. Shachkin and V. M. Shashkov]

[Text] The characteristics of the active medium of a $CO_2$ laser, excited by a non-self-sustained combined discharge with ionization of the medium by short electric pulses in a flow of a $CO_2$-$N_2$-He flow, were investigated. The dependence of the maximum energy contribution, amplification factor and heating of the gas on the composition of the mixture were measured. It is shown that a specific energy contribution of approximately 450 J/g with excitation efficiency of nitrogen and carbon dioxide oscillations of approximately 90 percent can be realized with the pumping method used.

Investigating the characteristics of a non-self-sustained combined discharge (NKR) with ionization of the medium by short electric pulses [1, 2] showed the promise of its application for pumping the working media of fast-flow gas lasers. The NKR with large gap realized in [2] is of especially great interest for development of powerful closed-cycle production $CO_2$ lasers. However, the dependence of the maximum energy contribution on the carbon dioxide concentration was not investigated in [2], the problem of the energy balance in the discharge was left open and the comparatively low dimensions of the investigated discharge chamber (RK) did not permit the use of the results obtained in developing the use of the results obtained in developing large-size installations. Moreover, the amplification factor of a weak signal, knowledge of which is necessary when designing a cavity, was not measured in [2]. The purpose of this paper was detailed investigation of the active medium excited by the NKR to justify the use of the given pumping method in production $CO_2$ lasers.

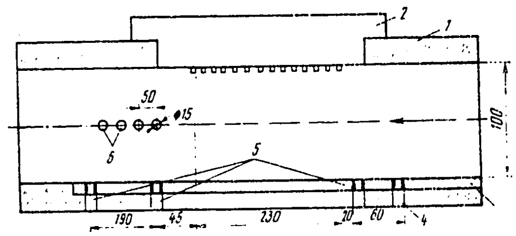


Figure 1. Diagram of Discharge Chamber: 1 -- housing; 2 -- cathode plate; 3 -- anode; 4 and 5 -- drain openings for measuring static pressure; 6 -- openings for measuring $K_{US}$. The arrow indicates the direction of pumping; the dimensions are given in millimeters.

Investigations were conducted in an RK, shown schematically in Figure 1. The discharge in it was accomplished so that the direction of the electron flow was perpendicular to the gas flow (the electrode system and the circuitry of the RK power supply are similar to those used in [2]). The anode was a flat copper plate and the cathode plate was made in the form of a block of copper rods 3 mm in diameter, built into the insulating plate with spacing of 10 mm. The block consisted of 14 rows of rods at right angles to the flow and there were 24 rods in each row. The distance between the anode and cathode plate comprised 100 mm, i.e., the volume of the discharge zone was approximately 3.4 liters. Each rod had an individual balanced resistor of approximately 2.7 kohms. The RK power supply was from a stationary regulated voltage source and 100-ns voltage pulse generator with recurrence frequency up to 20 kHz. The gas mixture was pumped by a vacuum pump system.

The integral electric characteristics of the discahrge were measured by extended methods, the gas heating in the RK was measured by the "gas-dynamic thermometer" method [3] and the amplification factor was determined by probing the active medium with the signal of a stable test laser operating in the center of one of the lines of the P- or R-branch in the band of 10.6 microns. The $CO_2$:$N_2$:He = $X_{CO_2}$:0.5:0.5 mixture was mainly investigated and in this case the carbon dioxide concentration $X_{CO_2}$ varied from 0 to 0.04 (in volume parts). The pressure of the mixture at the input to the discharge zone comprised 45 mm Hg and the flow velocity was 60 m/s.

The maximum energy contribution was determined by transition of the discharge to the inhomogeneous combustion stage. The dependence of the maximum energy contribution on the recurrence frequency of the ionizing pulses f and the current density in the pulse $f_i$ was investigated. The investigations showed that the first of these functions has a sloping maximum which shifts toward the low frequencies with an increase of current in the pulse. The typical dependence of the value of the volume-averaged discharge zone of the maximum energy contribution W/G (here $W = I(U - \Delta U)$ is the power contributed to the positive column of the glow discharge, U is the voltage in the discharge gap, I is the discharge current, $\Delta U = 300$ V is the sum of pre-electrode potential drops [1] and G is the flow rate of the mixture through the discharge zone) on the recurrence frequency of the ionizing pulses at different values of $j_i$ is presented in Figure 2. The maximum specific energy contribution of 450 J/g was achieved at $j_i = 0.45$ A/cm$^2$ and f = 3 kHz.

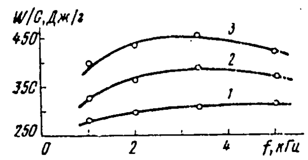


Figure 2. Dependence of Maximum Energy Contribution on Ionizing Pulse Recurrence Frequency at $j_i$ = 0.15 (1), 0.3 (2) and 0.45 (3) A/cm$^2$; $CO_2:N_2:He$ = 0.017:0.5:0.5 Mixture.

The dependence of the maximum energy contribution on the $CO_2$ molecule concentration was investigated at a frequency of f = 2kHz and $j_i = 0.3$ A/cm$^2$ (Figure 3). It was found that the maximum energy contribution W/G drops linearly with an increase of $X_{CO_2}$; for example, it is equal to 410 and 330 J/g, respectively, at $X_{CO_2}$ = 0 and 0.025. It should be noted that although the utilized pumping system did not permit investigation of the maximum energy characteristics at higher pumping rates, the results of [1] permit one to hope that an increase of flow velocity (at least up to 150 m/s) essentially does not change the value of the maximum energy contribution W/G.

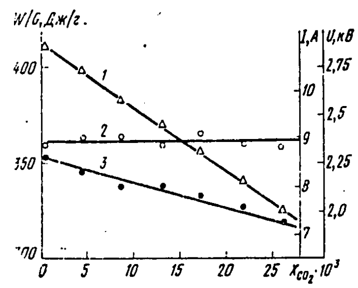


Figure 3. Dependence of Maximum Characteristics of Discharge W/G (1), U (2) and I (3) on $CO_2$ Concentration at $j_i = 0.3$ A/cm$^2$ and f = 2 kHz.

The main measurements of the amplification factor were made in the cross-section lagging 45 mm behind the last row of cathode rods (see Figure 1) over a wide range of working parameters. Gas heating was measured at the same time in this cross-section. The amplification factor increased monotonically with an increase of W/G (for example, $K_0 = 0.45\ m^{-1}$ for $X_{CO_2} = 1.7$ percent and W/G = 350 J/g) and while slightly dependent on the value of E/N (E is the mean electric field intensity in the discharge and N is the total particle density) in the investigated range of $E/N = (0.8-1.5)\cdot 10^{-16} V\cdot cm^2$. For practical purposes the experimental function $K_0(W/G)$ with an error not exceeding approximately 20 percent can be approximated in the range of W/G = 50-350 J/G by a straight line $K_0 = \alpha \cdot W/G$, where $\alpha = \alpha(X_{CO_2})$ (Figure 4). The tendency toward saturation observed in this figure is related to the increasing role of relaxation processes.

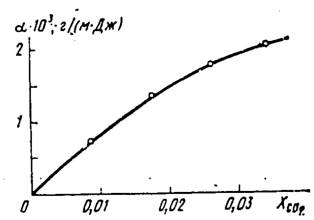


Figure 4. Dependence of Coefficient $\alpha = K_0 G/W$ on $CO_2$ Concentration.

Simultaneous measurements of the amplification factor and gas heating made it possible to determine the energy stored in the nitrogen oscillations and the $CO_2$ antisymmetrical mode. The following expression was used in the calculations for the amplification factor on the P-branch of the 10.6-micron band:

$$K_0,\ [\text{м}^{-1}] = B\frac{2JX_{CO_2}}{\Sigma X_i A_{c-i}}\frac{\exp[-0,5588\,J\,(J-1)/T]}{ZT^{3/2}}\left[\frac{e_3}{(1+e_3)}-\exp\left(-\frac{1,12J}{T}\right)\times\right.$$
$$\left.\times\left(\frac{e_2}{2+e_2}\right)^2\right],$$

where J is the rotational quantum number, T is gas temperature, $X_i$ is the concentration of the i-th component of the mixture, $A_{c-1}$ is the relative impact broadening coefficients of the i-th component of the oscillatory-rotational line, $Z^{-1}=16(1+e_2)/[(1+e_3)(2+e_2)^4]$ is the oscillatory statistical sum and $e_3$ and $e_2$ are the mean quantum numbers in the antisymmetrical and deformation modes of the $CO_2$ molecule. The presence of a large amount of helium in the mixture permitted the use of the oscillatory temperature of the deformation mode equal to gas temperature; at the same time it was assumed that the mean quantum number in the antisymmetrical mode of the $CO_2$ is equal to the mean quantum number in the $N_2$. Coefficients $A_{c-i}$ were taken as equal to 0.75 for nitrogen [4] and 0.69 for helium [5]. The significance of coefficient $P = 0.31\cdot 10^5$ was determined on the basis of data on resonance absorption of emission at the center of the P-20 line of the 00°1-10°0 transition of $CO_2$ in the atmosphere [6] (the absorption coefficient in the atmosphere of $0.072\ km^{-1}$ at 300°K was used).

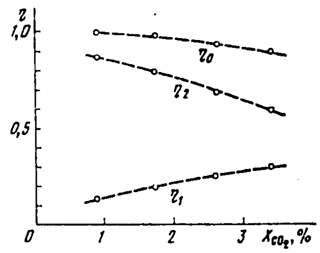


Figure 5. Dependence of Energy Distribution at Distance of 45 mm from the Discharge Zone Down the Flow on $CO_2$ Concentration.

The results of processing the experimental data, carried out near the maximum value of parameter $E/N = 1.25 \times 10^{-16}$ V·cm$^2$ (maximum energy contribution of 250 J/g), are presented in Figure 5. The error in measuring the value of $K_0$ did not exceed 5 percent in this case (the error in determination of $K_0$ increases due to its smallness at small values of the maximum energy contribution). In Figure 5, $\eta_1$ is the fraction of energy contributed to the positive discharge column, expended on gas heating to the cross-section in which $K_0$ is measured and $\eta_2$ is the fraction of energy stored in the nitrogen oscillations and in the $CO_2$ antisymmetrical mode, found from measuring $K_0$. It is obvious that the value of $\eta_0 = \eta_1 + \eta_2$ is approximately constant (within the range of measurement error of approximately 10 percent) and is close to unity; this indicates that the processes which lead to gas heating and excitation of nitrogen oscillations and of the $CO_2$ antisymmetrical mode exhaust all possible energy loss channels in the discharge. We note that the value of $\eta_0$ decreases somewhat with an increase of $CO_2$ concentration, which may indicate the increasing role of an energy loss channel not taken into account in our consideration, but this variation is within the range of measurement error and we cannot reliably judge it.

Measurements of profile $K_0$ down the flow and of gas heating beyond the discharge zone permitted determination of the relaxation time of the oscillatory energy stored in the $N_2$ molecules and the $CO_2$ antisymmetrical mode by two independent methods. For example, it comprised 8.6 ms for the $CO_2:N_2:He = 0.017:0.5:0.5$ mixture, which is somewhat higher than the values calculated by the data for $CO_2$ relaxation in $N_2$ and He, known from the literature [7]. The use of the measured relaxation rate of vibrational energy permits one to estimate which part of the discharge energy went to excitation of $N_2$ oscillations and the $CO_2$ antisymmetrical mode, but relaxed to heat to the cross-section in which $K_0$ is measured, and restoration of the effective value of efficiency $\eta_k$, i.e., the fraction of power contributed in the discharge to excitation of nitrogen oscillations and the $CO_2$ antisymmetrical mode useful from the viewpoint of laser efficiency (according to our data, $\eta_k = 0.9 \pm 0.05$ at $E/N = 1.25 \cdot 10^{-16}$ V·cm$^2$).

Thus, the energy balance in a non-self-sustained discharge was investigated experimentally as a result of the conducted work. It is shown that the processes which lead to direct gas heating and excitation of oscillations of nitrogen and the $CO_2$ antisymmetrical mode exhaust the energy loss channels in the plasma of a non-self-sustained discharge in a $CO_2$-$N_2$-He laser mixture and the vibrational efficiency of the discharge exceeds 90 percent under typical experiment conditions. The integral characteristics of the active medium were investigated. The possibility of achieving specific energy contributions at the level of 400-450 J/g is shown on an example of a model of a production $CO_2$ laser and the amplification factor of a weak signal was measured over a wide range of operating conditions. The scale of the conducted experiments permits the use of the derived data to design powerful production $CO_2$ lasers based on the given pumping method.

## BIBLIOGRAPHY

1. Naumov, V. G. and V. M. Shashkov, KVANTOVAYA ELEKTRONIKA, Vol 4, 1977.

2. Napartovich, A. P., V. G. Naumov and V. M. Shashkov, PIS'MA V ZhTF, Vol 3, 1977.

3. Vedenov, A. A. A. F. Vitshas et al, Vol 14, 1976.

4. Patty, R. R. et al, APPL. OPTICS, Vol 7, 1968.

5. Danilov, V. V. et al, ZHURN. PRIKL. TEKH. I TEKHN. FIZ., No 6, 1972.

6. Aref'yev, V. N. and N. I. Sizov, KVANTOVAYA ELEKTRONIKA, Vol 4, 1977.

7. Losev, S. A. and V. N. Makarov, KVANTOVAYA ELEKTRONIKA, Vol 1, 1974.

[156-6521]



6521
CSO: 1862

ELECTRICITY AND MAGNETISM

UDC621.378.324

THE MECHANISM OF DIRECT HEATING OF A $CO_2$-$N_2$-He LASER MIXTURE IN A NON-SELF-SUSTAINED DISCHARGE

Moscow KVANTOVAYA ELEKTRONIKA in Russian Vol 6 No 7, Jul 1979 signed to press 27 Oct 78 pp 1446-1451

[Article by I. V. Kochetov, V. G. Naumov, V. G. Pevgov and V. M. Shashkov]

[Text] The results of experiments to determine the fraction of energy contributed to direct heating of a $CO_2$-$N_2$-He laser mixture under conditions typical for a non-self-sustained flow discharge, and calculation-theoretical analysis of the possible electron energy loss channels which lead to direct heating are presented. A new value is found for the excitation cross-section of the $01^10$ level of the $CO_2$ molecule by electron impact.

Interest in study of a glow discharge in the flow of a laser mixture was increased with regard to active development of investigations in laser technology. Calculated data found by solving the Boltzmann equation for the electron distribution function are usually employed when analyzing the electron energy losses in the plasma of a glow discharge (see, for example, [1]). This problem has been little investigated experimentally.

The purpose of this paper was experimental determination of the energy fraction contributing to direct heating of the $CO_2$-$N_2$-He laser mixture under conditions typical for a non-self-sustained glow discharge and calculation-theoretical analysis of the possible electron energy loss channels which lead to direct gas heating.

The experiments were conducted on a model of the discharge chamber of a fast-flow continuous $CO_2$ laser with combined discharge pumping of the laser mixture [2]. The use of a combined discharge made it possible not only to increase the specific energy contribution compared to pumping by a self-sustained discharge, but also to regulate the electron temperature at given electron concentration. The discharge chamber was a rectangular channel with cross-section of 100X200 mm with electron system in it similar to that used in [2]. The anode was a flat copper plate 20 cm wide and 50 cm long. The cathode was made in the form of a body of copper rods built into the dielectric plate with spacing of 1 cm (14 rows at right angles and 24 rows along the flow). The interelectrode gap was 10 cm. The main measurements were made in a $CO_2:N_2:He = X_c:0.5:0.5$ mixture, where $X_c$ varied from 0 to 0.04 (in parts by volume). The pressure of the mixture at the input to the discharge zone comprised 45 mm Hg and the flow velocity comprised 60 m/s.

It is known [1] that the energy contributed to the positive column of a glow discharge is distributed in a $CO_2$-$N_2$-He mixture along the following main channels: 1) elastic electron and ion scattering on helium atoms and $N_2$ and $CO_2$ molecules; 2) electron scattering on $N_2$ and $CO_2$ molecules with excitation of rotational states; 3) excitation of vibrational levels of the symmetrical and deformation modes of the $CO_2$ molecule by electron impact; 4) excitation of the vibrational levels of the $N_2$ molecule and of the asymmetrical mode of the $CO_2$ molecule by electron impact; and 5) excitation of the electron levels of $N_2$, He and $CO_2$ by electron impact. The electron energy losses through channel 1 lead directly to gas heating. Since the rotational relaxation times on the order of gas-kinetic and the relaxation time of the energy stored in the symmetrical and deformation modes are much less under our conditions than the gas transit time through the discharge zone due to rapid relaxation of the $01^10$ level of the $CO_2$ molecule upon collision with helium [3], channels 2 and 3 also lead to gas heating in the discharge zone. The energy stored in the vibrational levels of the $N_2$ molecules and the asymmetrical mode of the $CO_2$ molecule is converted to heat under our conditions due to the collision relaxation during times on the order of the gas transit time through the discharge zone, so that gas heating through channel 4 may be assumed slow. The electron energy losses through channel 5 at typical values of $E/N < 2\cdot10^{-16}$ V$\cdot$cm$^2$ (E is the electric field intensity and N is the gas concentration at the input to the discarge zone) for our conditions can be disregarded [1]. Thus, under our conditions the energy contributed to the gas through channels 1-3 is completely converted to heat in the discharge zone and leads to direct (instantaneous) gas heating in the discharge, while channel 4 leads to slow gas heating both in and beyond the discharge zone (down the flow). This difference in the typical heating times was used to determine the energy fraction contributing to direct gas heating.

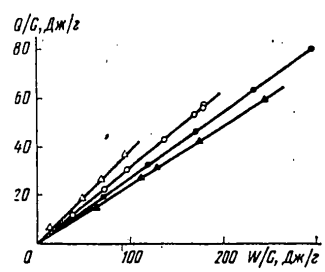


Figure 1. Dependence of Specific Gas Heating in Discharge Zone A/G on Specific Energy Contribution W/G ($X_C$ = 0.017)

Gas heating in the discharge zone (based on $L_1$ = 28 cm) and beyond it (based on $L_2$ = 19 cm) was measured by the gas-dynamic thermometer method [4]. The use of a combined discharge made it possible to conduct measurements in the region of $E/N = (0.6\text{-}1.6)\cdot 10^{-16}$ V·cm$^2$ at different levels of the specific energy contribution to the positive problem in the non-self-sustained discharge phase (up to 350 J/g). Gas heating due to pulsed discharge was low and was taken into account similar to [5]. The sum of the pre-electrode potential drops was assumed equal to 300 V.

The power Q contributing to gas heating was calculated by the formula derived on the same assumptions as in [5]:

$$\frac{Q}{G} = \frac{S^2}{G^2}\, p_1\, \Delta p \Sigma \frac{X_i \gamma_i}{\gamma_i - 1}, \qquad (1)$$

where S is the discharge cross-section with respect to flow, G is the flow rate of the mixture through the discharge zone, $p_1$ is the pressure at the input to the discharge zone, $\Delta$ p is the static pressure drop during deduction of the drop caused by friction and heating by a pulsed discharge, $X_i$ is the relative concentration of the i-th component of the mixture and $\gamma_i$ is the index of the adiabatic curve.

The dependence of the value of specific gas heating in the discharge zone Q/G on the specific energy contribution W/G (W is the power contributed to the positve column in the non-self-sustained discharge phase) at different values of E/N is presented in Figure 1. The gas temperature at the input to the discharge zone was maintained at 273 $\pm$ 3°K. The investigations showed that the dependence of Q/G (W/G) is linear within the range of measurement accuracy (the error of a single measurement $\leqslant$ 10 percent) over the entire investigated range of W/G and E/N despite variation of the gas temperature along the length of the discharge zone. Gas heating in the discahrge zone leads, on the one hand, to an increase of E/N along the flow (up to 15-20 percent at maximum values of W/G) and to a corresponding decrease of direct heating (see below) and, on the other hand, it leads to an increase (by 10-15 percent at the maximum) of the relaxation rate of the energy stored in the vibrational degree of freedom of $N_2$ and the asymmetrical $CO_2$ vibrational mode and to the corresponding increase of gas heating along channel 4. These two effects are minor under our conditions and have the same different sign which leads to the linear function Q/G (with accuracy up to 10 percent) in Figure 1. The value of $\eta_1$ = Q/W, determined by the slope of straight line Q/G(W/G) is related both to large values of W/G (200-300 J/g) and to small values ($\leqslant$ 100 J/g) at which the effect of gas temperature variation on the heating rate can be previously disregarded. Therefore, one may assume that the values of $\eta_1$ calculated from Figure 1 are related to the values of E/N, determined at the input to the discharge zone. The dependence of $\eta_1$ on E/N found in this manner is presented in Figure 2.

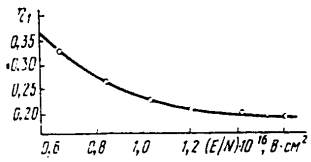


Figure 2. Dependence of Fraction of Power Contributing to Gas Heating in Discharge Zone on the Given Field Intensity ($X_C$ = 0.017)

The dependence of the fraction of power $\eta_2$ contributing to gas heating beyond the discharge zone based on $L_2$ on the value of E/N, determined in a similar manner, is presented in Figure 3. We note that $E_2$ was determined in modes when the total heating based on $L_1 + L_2$ did not exceed 40°K, so that variation of the relaxation rate caused by variation of gas temperature apparently did not exceed 5 percent. Then the fraction of power contributing to gas heating in the discharge zone and based on $L_2$ can be determined by the following relations:

$$\eta_1 = 1 - (1-\eta_0)\frac{v\tau_p}{L_1}\left[1 - \exp\left(-\frac{L_1}{v\tau_p}\right)\right], \quad (2)$$

$$\eta_2 = (1-\eta_1)\left[1 - \exp\left(-\frac{L_2}{v\tau_p}\right)\right], \quad (3)$$

where $\eta_0$ is the fraction of power contributing to direct gas heating, v is the flow velocity and $\tau_r$ is the relaxation time of the vibrational degrees of freedom of $N_2$ and the $CO_2$ asymmetrical vibrational mode.

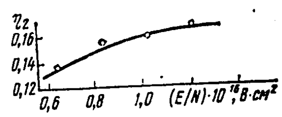


Figure 3. Dependence of Fraction of Power Contributing to Gas Heating Beyond the Discharge Zone on the Given Field Intensity ($X_C$ = 0.017)

The measurements showed that $\eta_2/(1 - \eta_1)$, as one would expect, does not depend on E/N over the entire investigated range, which made it possible to calculate the rate of energy relaxation contributed to the gas along channel 4, determined under our conditions by the rate of quantum exchange of the asymmetrical mode of the $CO_2$ molecule for quanta of the symmetrical and deformation modes during collisions with He atoms and $N_2$ molecules. The rate constant which we determined for this process $(p\tau_r)^{-1} = 0.035$ $(\text{microns}\cdot\text{atm})^{-1}$, which is somewhat below the known [6] values of the quantum exchange rate during collisions of $CO_2$ molecules with both helium and nitrogen.

Utilizing the value of $\tau_r$ which we determined, one can calculate the fraction of the power contributing to direct heating and which is the sum of the energy losses to elastic collisions and excitation of rotations and lower vibrational levels of the $CO_2$ molecule.

We made numerical calculations using a computer to determine the relative contribution of different channels to the observed direct heating of the investigated mixtures in an electric discharge. Analysis of the heating channels was made on the basis of solving the Boltzmann equation for the electron energy distribution function under conditions of an electric discharge plasma.

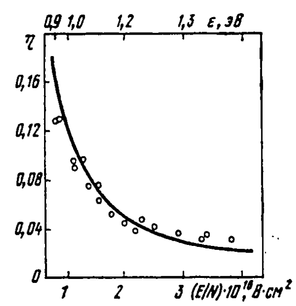


Figure 4. Dependence of Fraction of Power Contributing to Direct Gas Heating on the Given Field Intensity for Nitrogen: O -- experiment; solid line -- calculation

It should be noted that the main component of the mixtures considered in the given paper is nitrogen; therefore, we attempted to achieve better agreement of the calculated and observed value of gas heating under conditions of an electric discharge in nitrogen than occurred in our previous investigations [5, 7]. The main direct heating channel under these conditions is the process of rotational excitation of the nitrogen molecule. Whereas it was difficult to select a more reliable value than that obtained on the basis of the Fisk model potential [8] for the excitation cross-section of nitrogen molecule rotations by the moment the calculations were made [7], the situation is now changed. Comparison of the experimental and calculated values of direct gas heating in an electric discharge in nitrogen when the calculated value from [9] was selected for the excitation cross-section of the nitrogen molecule rotations is presented in Figure 4. Good agreement of calculation with experiment indicates the correctness of this selection.

Addition of helium to the nitrogen in the range of low values of E/N leads to additional gas heating due to elastic energy losses by the electrons of the gas-discharge plasma in the helium atoms. The heating channels in the $N_2$:He = 1:1 mixture are presented in Figure 5.

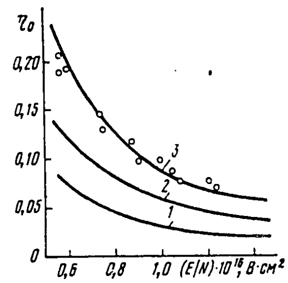

Figure 5. Dependence of Fraction of Power Contributing to Direct Gas Heating on the Given Field Intensity for the $N_2$:He = 1:1 Mixture: O -- experiment; solid lines -- calculation of elastic losses (1), losses to rotational excitation (2) and their sum (3)

An additional heating channel appears under our conditions in a ternary mixture containing $CO_2$ due to rapid relaxation of the lower vibrational levels of the $CO_2$ molecules, excited in the discharge by electron impact (Figure 6). The values from [10], with the exception cross-section of the $01^10$ vibrational level, were used in the calculations from the excitation cross-sections of the $CO_2$ molecules. The energy dependence obtained in Born approximation was used in [10] for this value, but it was noted that there is some arbitrary selection of the shape of this cross-section in the energy range from threshold to 3 Ev which does not contradict the existing experimental data.

Systematic underestimation of the value of heating compared to experiment in the range of low values of parameter E/N (the dashed line in Figure 6) was observed in our calculations in the case where all the cross-sections were taken from [10]. This underestimation exceeds the value of experimental error and can be explained by the underestimated value of the excitation cross-section of the $01^10$ level near the threshold energy values. To explain our experiments, the shape of the excitation cross-section of the $01^10$ level of the $CO_2$ molecule should be close to that given in Figure 7 (curve 3). To determine the excitation cross-section of the $CO_2$ level ($01^10$) upon electron impact, besides the requirement of matching of the calculated an measured values of heating, the requirement of matching the calculated and measured values of the kinetic electron coefficients in the plasma of an electric discharge in pure $CO_2$ was also applied. Detailed analysis of the experimental values of the kinetic electron coefficients for this case is given in [10].

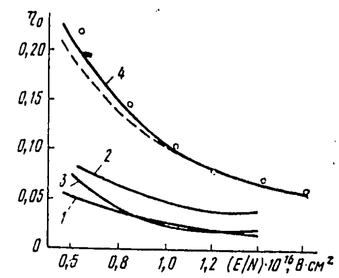


Figure 6. Dependence of Fraction of Power Contributing to Direct Gas Heating on the Given Field Intensity for the $CO_2:N_2:He = 0.017:0.5:0.5$ Mixture: O -- experiment; dotted lines -- calculation with new excitation cross-section of $01^10$ level; 1 --elastic losses; 2 -- losses to rotational excitation; 3 -- losses to excitation of lower $CO_2$ levels; 4 -- sum of 1, 2, and 3; dashed line -- total gas heating with cross sections for $CO_2$ from [10]

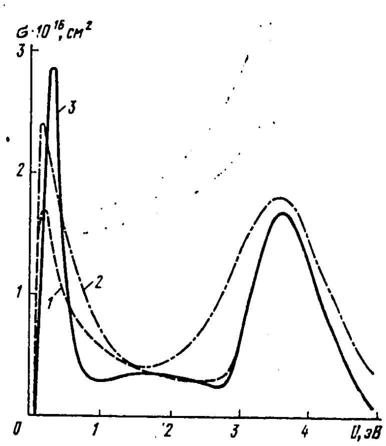


Figure 7. Excitation Cross-Section of $01^10$ Level of $CO_2$ Molecule From [10] -- (1); [14] -- (2); from the given paper -- (3)

It is interesting to note that cross-sections having a typical peak in the prethreshold energy range were found in experimental papers [11-13] where the excitation cross-section of the vibrational mode of the dipole molecules was investigated. General principles are obvious in the shapes of these cross-sections and those which we found (see Figure 7). However, the $CO_2$ molecule has no dipole moment in the ground state, whereas it has a large induced dipole moment. Hence, one may assume that similar principles in the shape of the excitation cross-sections of the vibrational levels, besides dipole molecules [11-13], are also inherent to the molecules having large induced dipole moment. However, this hypothesis requires further experimental and theoretical checking.

The calculated results for heating in a mixture containing 1.7 percent $CO_2$ (see Figure 6) were found with a new excitation cross-section of the $CO_2$ level ($01^10$). The measurements made at different values of $CO_2$ concentration showed that qualitatively the function $\eta_0(E/N)$ varies insignificantly over the entire investigated range of $X_C$ = 0-0.04 (and the values themselves of $\eta_0$ at fixed value of E/N). Thus, one may conclude that the vibrational efficiency of a non-self-sustained discharge in mixtures with low $CO_2$ content (less than 5 percent) exceeds the value of 90 percent at $E/N \geqslant 10^{-16}$ $V \cdot cm^2$, decreasing appreciably with a decrease of E/N.

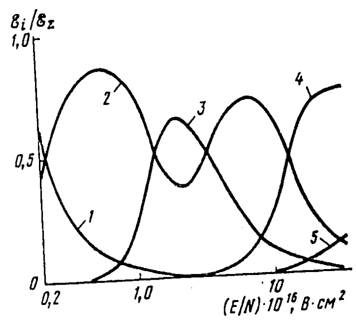


Figure 8. Relative Electron Energy Losses in the Discharge Plasma in $CO_2$ to Excitation of Rotations (1), mnO Modes (2), The 001 Level (3), Electron States (4) and to Ionization (5)

Rotational excitation processes of $CO_2$ molecules, which were previously disregarded (see [10] and the references in it) may have an appreciable effect on the energy balance at large $CO_2$ concentrations and low values of parameter E/N. The energy balance in a gas-discharge $CO_2$ plasma with regard to rotational excitation of the molecules is presented in Figure 8. The results of [9] were used in the calculation for the rotational excitation cross-section of $CO_2$ molecules upon electron impact. The calculations are valid on the assumption of $1 - T/T_e \not\approx 1$ (T is gas temperature and $T_e$ is electron temperature). It is obvious that the rotational excitation of $CO_2$ molecules by electron impact must be taken into account at a value of parameter $E/N \leq 10^{-16}$ $V \cdot cm^2$.

In conclusion, the authors express gratitude to A. P. Napartovich for initiating the given investigation and useful discussions and to L. V. Shachkin for assistance in conducting the experiments.

BIBLIOGRAPHY

1. Nighan, W. L., PHYS. REV. A., Vol 2, 1970.

2. Naumov, V. G. and V. M. Shashkov, KVANTOVAYA ELEKTRONIKA, Vol 4, 1977.

3. Taylor, R. L. and S. Bitteman, REV. MOD. PHYS., Vol 41, 1969.

4. Vedenov, A. A., A. F. Bitshas, V. Ye. Gerts and V. G. Naumov, TVT, Vol 14, 1976.

5. Napartovich, A. P., V. G. Naumov and V. M. Shashkov, DAN SSSR, Vol 232, 1977.

6. Losev, S. A. and V. N. Makarov, KVANTOVAYA ELEKTRONIKA, Vol 1, 1974.

7. Karlov, N. V., Yu. B. Konev, I. V. Kochetov and V. G. Pevgov, FIAN Preprint No 91, Moscow, 1976; Yu. B. Konev, I. V. Kochetov, V. S. Marchenko and V. G. Pevgov, KVANTOVAYA ELEKTRONIKA, Vol 4, 1977.

8. Oksyuk, Yu. D., ZHETF, Vol 49, 1965.

9. Morrison, M. A. and N. F. Lane, PHYS. REV., Vol 16, 1977.

10. Pevgov, V. G., Candidate Dissertation, MFTI, 1977.

11. Rohr, K. and F. Linder, J. PHYS. B.; ATOM. MOLEC. PHYS., Vol 9, 1976.

12. Seng, G. and F. Linder, J. PHYS. B.; ATOM. MOLEC. PHYS., Vol 9, 1976.

13. Rohr, K.k J. PHYS. B.; ATOM. MOLEC. PHYS., Vol 10, L399, 1977.

14. Lowke, J. J., A. V. Phelps and V. W. Irwin, M. APPL. PHYS., Vol 44, 1973.
[156-6521]



6521
CSO: 1862

ELECTRICITY AND MAGNETISM

UDC621.378.33

# THE CHAIN MECHANISM OF EXCITING A CONTINUOUS CHEMICAL HF LASER WITH CYLINDRICAL NOZZLE

Moscow KVANTOVAYA ELEKTRONIKA in Russian Vol 6 No 7, Jul 1979 signed to press 5 Nov 78 pp 1476-1483

[Article by A. A. Stepanov and V. A. Shcheglov, Physics Institute imeni P. N. Lebedev of the USSR Academy of Sciences, Moscow]

[Text] Based on solution of the Navier-Stokes equations for a chemically reacting mixture (in approximation of the boundary layer), the characteristics were investigated with regard to the vibrational processes and radiation kinetics and the energy capabilities of a continuous chemical HF laser with cylindrical nozzle were analyzed in the case of realizing the chain excitation mechanism. It is shown that selection of the optimum configuration of the ring model during chain pumping permits one 1) to significantly neutralize the thermal effect and to accomplish transition to higher static pressures in the cavity zone; 2) to realize very high specific-energy laser parameters; and 3) to appreciable increase the efficiency of the laser-energy complex as a whole.

## 1. Introduction

The majority of papers on continuous chemical lasers based on hydrogen halides was until the present devoted to supersonic HF(DF) lasers with single-act excitation process $F + H_2(D_2) \rightarrow HF(DF) + H(D)$ (the "cold" reaction mechanism). The specific laser energy of these installations exceeds 100 J/g (see, for example, [1-3]). The energy capabilities of supersonic hydrogen fluoride lasers based on the "cold" reaction are even now not exhausted [4], but the prospects for development of this class of systems is related to accomplishing the chain excitation mechanism [5-8]:

$$F+H_2\rightarrow HF(v)+H, \quad -\Delta H_1=31{,}7 \text{ kcal/mole;} \qquad (1)$$

$$H + F_2 \rightarrow HF(v) + F, \quad -\Delta H_2 = 97,9 \text{ kcal/mole} \tag{2}$$

The first successful experiments on realization of chain pumping have a continuous HF laser (with flat design of the nozzle) were reported in [9, 10]. Specifically, a specific laser energy level above 300 J/g was achieved in [10].

The chain process (1) and (2) is attractive primarily due to the fact that the potential reserve of the chemical energy released in the form of vibrational energy of excited HF molecules when it is accomplished exceeds that in the case of single-act pumping reaction (1). In this case the "hot" reaction (2) becomes dominant in the energy sense. It follows from the foregoing that in the case of a continuous HF laser based on the chain reaction, one can essentially expect an appreciable increase of the specific energy parameters. However, there are specific difficulties in the path of developing this laser [5, 8]. One of them is related to the significant heat release in the cavity zone and because of this to the possibility of significant temperature and pressure gradients occurring. The latter circumstance may lead to closing of the supersonic channels (flow "crisis") and interruption of generation [8]. Neutralization of the thermal effect requires adoption of special measures: the use of intermediate diluent jets, spatial separation of the oxidizer and fuel jets and so on.

The characteristics were investigated in the energy capabilities of the continuous chemical HF laser with cylindrical nozzle and chain excitation mechanism were analyzed for the first time in the given paper. It is shown that the ring model with optimum configuration, neutralizing to a significant degree the thermal effect in the cavity zone, permits one to realize very high energy parameters of this HF laser.

## 2. Manifestation of the Thermal Effect in a Supersonic Flow. Estimates for a Chemical HF Laser.

Qualitative consideration of the "thermal crisis" phenomenon can be made within the framework of a single-dimensional model, which describes a supersonic flow with premixed reagents. The equation for the Mach number M of the flow in the channel with variable cross-section S(x) in the presence of thermal sources has the form [11]

$$\frac{1}{M^2}\frac{dM^2}{dx} = \frac{1+\gamma M^2}{1-M^2}\left(\frac{1}{H}\frac{dQ}{dx} - \frac{1}{S}\frac{dS}{dx}\right) - \frac{1}{S}\frac{dS}{dx}, \tag{3}$$

where x is the coordinate along the flow axis, $\gamma = c_p/c_v \approx$ const, $c_p$ and $c_v$ are the molar specific heats at constant pressure and volume, $H = c_pT/W$ is the enthalpy of the mixture, T is temperature, W is the molecular weight of the mixture and dQ/dx is the specific rate of heat release.

In the case of a section of constant cross-section (S = const), from (3) we find

$$\ln\left\{\frac{M^2}{M_0^2}\left(\frac{1+\gamma M_0^2}{1+\gamma M^2}\right)^{\frac{\gamma+1}{\gamma}}\right\} = \frac{W}{c_p}\int_0^x \frac{dQ(x)}{T}, \qquad (4)$$

where $M_0$ is the Mach number in the cross-section x = 0. The known statement follows from (4): the Mach number decreases ($M < M_0$) in the channel of constant cross-section upon approach of heat ($dQ > 0$) to supersonic flow ($M_0 > 1$). Making use of the relation $dQ \simeq c_v dT/W$, using (4) we find the relationship between T and M:

$$T/T_0 \simeq (M^2/M_0^2)^{\gamma}\,[(1+\gamma M_0^2)/(1+\gamma M^2)]^{\gamma+1}, \qquad (5)$$

where $T_0$ is the initial gas temperature at x = 0.

For the critical flow mode (corresponding to the "thermal cutoff" of the channel), one should assume M = 1 in (5), then

$$T_*/T_0 \simeq M_0^{-2\gamma}\,[(1+\gamma M_0^2)/(1+\gamma)]^{\gamma+1}. \qquad (6)$$

If the heat of reaction were determined in a fixed gas enclosed in a closed volume, the maximum heating temperature would be determined by the relation $c_v(T_{max} - T_0) = \xi_{ok} Q_0$, where $Q_0$ is the molar thermal effect of the reaction between the oxidizer ($F_2$) and the fuel ($H_2$) and $\xi_{ok}$ is the molar fraction of the oxidizer particles in the mixture provided that it is taken insufficiently with respect to the fuel (which is typical for continuous HF lasers). $T_* > T_{max}$ due to flow retardation in a supersonic flow with the same heat release. This circumstance permits us to determine the maximum permissible oxidizer concentration in the flow:

$$\xi_{ok}^* \leq \frac{c_v T_0}{Q_0}\left\{M_0^{-2\gamma}\left(\frac{1+\gamma M_0^2}{1+\gamma}\right)^{\gamma+1} - 1\right\}. \qquad (7)$$

We note that condition (7) is softened somewhat when the final mixing rate of the reagents is taken into account. Let us consider two limiting cases:

1. In the case of "cold" pumping reaction (1), we have $Q_0 \approx 32$ kcal/mole. Having substituted the typical values $M_0 \approx 5$-7, $T_0 \approx 300$ K, $\gamma \approx 1.5$ and $C_v \approx 4$ cal/(mole·deg) in (7), we find $\xi_{ok}^* \lesssim 0.25$-0.5.

2. We have $Q_0 \approx 130$ kcal/mole with the chain mechanism of excitation (1) and (2). Having assumed that $M_0 \approx$ 5-7, $T_0 \approx 150$ K, $\gamma \approx$ 1.5 and

$c_v \approx$ 4 cal/(mole·deg), from (7) we have $\xi^*_{ok} \lesssim$ 0.035-0.07; consequently, the "thermal cutoff" mode may be observed in a supersonic flow at $\xi_{ok} >$ 0.035-0.07 and in this case one should expect a temperature increase to $T_* \gtrsim$ 1500 K.

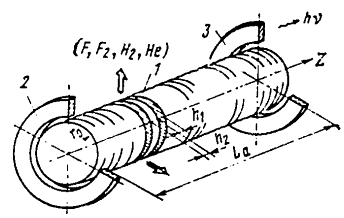


Figure 1. Simplified Diagram of Ring Model of a Continuous HF Laser: 1 -- cylindrical nozzle; 2 and 3 -- cavity mirrors

Relation (7), from the viewpoint of the occurrence of the critical mode, is essentially the condition which limits the chemical energy reserve in the flow. Having turned to equation (3), it is easy to see that the indicated constraint may be appreciably weakened if the possibility of expansion ($dS/dx > 0$) appears in the flow, for example during radial flow of the gas from a cylindrical nozzle (Figure 1). The subsequent sections of the paper are devoted to study of the ring model of a HF laser.

## 3. Gas Dynamics Equations

The cylindrical nozzle of a supersonic chemical HF laser includes a large set of coaxial small ring nozzles with alternating helium- and fuel-diluted ($H_2$) oxidizer jets (F and $F_2$); the flows travel in the radial direction and the cavity is formed by ring-shaped mirrors (see Figure 1). The geometric structure of the nozzle is determined by the cylinder radius $r_0$ and the heights $h_1$ and $h_2$ of the elementary ring nozzles for the oxidizer and fuel at $r = r_0$. The half-period of the cylinder block is determined by the relation $h_* = 1/2 (h_1 + h_2)$.

The gas dynamics equations in the cylindrical coordinate system (r, z) are written in the form (here we are limited by approximation of the boundary layer)

$$\frac{1}{r}\frac{\partial}{\partial r}(\rho u r) + \frac{\partial}{\partial z}(\rho v) = 0; \qquad (8a)$$

$$\rho u \frac{\partial u}{\partial r} + \rho v \frac{\partial u}{\partial z} = -\frac{dp}{dr} + \frac{\partial}{\partial z}\left(\mu \frac{\partial u}{\partial z}\right); \qquad (8b)$$

$$\rho u \frac{\partial h}{\partial r} + \rho v \frac{dh}{\partial z} = u \frac{\partial p}{dr} + \mu \left(\frac{\partial u}{\partial z}\right)^2 + \frac{\partial}{\partial z}\left(\lambda \frac{\partial T}{\partial z}\right) + \frac{\partial}{\partial z}\left(\rho \sum_i h_i D_i \frac{\partial C_i}{\partial z}\right) - \\ - \sum_v g^l_{v,\,v-1} I^{l}_{v,\,v-1}; \tag{8c}$$

$$\rho u \frac{\partial C_i}{\partial r} + \rho v \frac{\partial C_i}{\partial z} = \dot{w}_i + \frac{\partial}{\partial z}\left(\rho D_i \frac{\partial C_i}{\partial z}\right), \tag{8d}$$

where (8a) is the continuity equation, (8b) is the equation of motion, (8c) is the energy equation and (8d) is the continuity equation for individual components ($i = F, F_2, H, H_2$, He and HF(v), v = 0, 1,..., 8). The equation of state supplements system (8)

$$p = \rho RT/W. \tag{9}$$

The following notations are introduced in (8) and (9): u and v are the radial and axial components of the velocity vector; p, $\rho$ and T are flow pressure, density and temperature; $h = \sum_i h_i C_i$ is the specific enthalpy of the mixture; $C_i = \rho_i/\rho$ is the relative mass concentration of the i-th component; $w_i$ are the terms corresponding to the processes of chemical, vibrational and radiation kinetics; W is the molecular weight of the mixture; and $\mu$, $\lambda$ $D_i$ are the coefficients of dynamic viscosity, thermal conductivity and diffusion. See [4, 8, 12] for more detail about the structure of the individual terms, transfer coefficients and velocity constants of the processes. It is assumed in the given equations that diffusion is laminar in nature. The transverse pressure gradient ( $\partial p/\partial z = 0$) was disregarded in the calculations.

With numerical integration of equations (8) and (9), one may convert from cylindrical coordinates r and z to variables $\xi$ and $\psi$, utilizing the Mises transform [13]:

$$\xi = r, \; \psi = r_0^{-1} \int_h^z \rho u r dz. \tag{10}$$

With regard to (10), system (8) and (9) is transformed to the form

$$\psi_* = r_0^{-1} \int_0^{h_*} \rho u r dz = \text{const}; \tag{11}$$

$$\frac{\partial u}{\partial \xi} - \left(\frac{\xi}{r_0}\right)^2 \frac{\partial}{\partial \psi}\left(\rho u \mu \frac{\partial u}{\partial \psi}\right) = -\frac{1}{\rho u}\frac{dp}{d\xi}; \tag{12}$$

$$c_p \frac{\partial T}{\partial \xi} - \left(\frac{\xi}{r_0}\right)^2 \left\{\frac{\partial}{\partial \psi}\left(\rho u \lambda \frac{\partial T}{\partial \psi}\right) + \rho u \frac{\partial T}{\partial \psi}\left(\sum_i c_{p_i} \rho D_i \frac{\partial C_i}{\partial \psi}\right)\right\} = \dot{w}_T + \frac{1}{\rho}\frac{dp}{d\xi}; \tag{13}$$

$$p=\rho RT/W; \tag{14}$$

$$\frac{\partial C_i}{\partial \xi}=\left(\frac{\xi}{r_0}\right)^2\frac{\partial}{\partial \psi}\left(\rho^2\, uD_i\frac{\partial C_i}{\partial \psi}\right)+\frac{\dot{w}_i}{\rho u}. \tag{15}$$

See [4] with respect to the structure of term $\dot{w}_T$.

Equation (11) corresponds to the law of conservation of mass in integral form. Differentiating (11) with respect to $\xi$, taking (14) into account in this case and assuming that $\partial p/\partial \psi = 0$, it is easy to find

$$\frac{1}{p}\frac{dp}{d\xi}=\psi_*^{-1}\int_0^{\psi_*}\left(\frac{1}{T}\frac{\partial T}{\partial \xi}-\frac{1}{u}\frac{\partial u}{\partial \xi}-\frac{1}{W}\frac{\partial W}{\partial \xi}\right)d\psi-\frac{1}{\xi}. \tag{16}$$

System (12)-(14) and (16) is closed with respect to all the gas dynamic variables ($p$, $\rho$, $T$ and $u$) and is a system of integrodifferential equations, for solution of which iteration methods may be used.

The boundary conditions for the complete system of equations (12)-(16) are based on consideration of the periodicity of the flow structure with respect to the Z-axis:

$$\frac{\partial u}{\partial \psi}=\frac{\partial T}{\partial \psi}=\frac{\partial \rho}{\partial \psi}=\frac{\partial C_i}{\partial \psi}=0 \text{ at } \psi=0,\ \psi_*. \tag{17}$$

The conditions at the output from the nozzle, i.e., at $\xi = r_0$ have the form

$$u=u_0(\psi);\ T=T_0(\psi);\ \rho=\rho_0(\psi);\ p=p_0;\ C_i=C_i^0(\psi). \tag{18}$$

We shall not dwell on problems related to processes of chemical, vibrational and radiation kinetics (see [4, 8, 12]). Let us note only that, unlike [4], chemical pumping in the considered case includes two links of chain process (1) and (2). It is taken into account in this case that vibrational states with v = 1-3 are excited in reaction (1) and states with v = 1-8 are excited in (2). As in [4], it was assumed that the rotational degrees of freedom of the HF molecules are in equilibrium with the foreward degrees of freedom.

## 4. Initial Data

The following parameters were fixed in the calculations: nozzle radius $r_0$, the heights of the ring nozzles $h_1$ and $h_2$, initial pressure $p_0$, the degree of helium dilution of the oxidizer $\beta_{He} = [He]/[F_2]_0$, the degree of fluorine dissociation $\alpha_F$, initial pressure, temperature and velocity of the oxidation ($p_1$, $T_1$ and $u_1$) and reaction ($p_2$, $T_2$ and $u_2$) flows and the threshold amplification factor $g_p$. The following values were taken in typical calculations for the indicated parameters: $h_1/h_2 = 2$, $h_* = 1/2\ (h_1 + h_2) = 0.25$ cm, $p_0 = p_1 = p_2 = 15$ mm Hg, $T_1 = 150$ K, $T_2 = 160$ K, $u_1 = u_2 = 2.5$ km/s, $\beta_{He} = 10$, $\alpha_F = 15$ percent and $g_p = 10^{-3}$ $cm^{-1}$. The nozzle radius $r_0$ varied within the range of 5-50 cm. In some calculations $p_0$ and the degree of oxidizer dilution $\beta_E$ also varied. The characteristics of the calculating method are also considered in [4].

## 5. Results of Calculations

The main results of solving the problem formulated above are presented in the given section. Figures 2 and 3 illustrate the variation of the mean values of the gas dynamic flow parameters with respect to the period of the nozzle structure in the cavity zone: temperature $T_*$, pressure $p_*$, velocity $u_*$ and Mach number $M_*$, and in this case the curves for $T_*$ and $p_*$ are given in the absence of a cavity at $\beta_{He} = 15$ for retention of the general scale (we note that a flow crisis is possible in the absence of a cavity from calculations at $\beta_{He} \approx 10$ and $r_0 > 10$ cm, but it is completely eliminated by a powerful radiation field right up to $r_0 \lesssim 20$ cm). As can be seen from Figures 2 and 3, variation of the design configuration and the composition of the mixture has an appreciable effect on the distribution of the flow parameters in the active zone. The factor of radial expansion plays an important role at relatively small nozzle radii ($r_0 \lesssim \Delta r_1$, $\Delta r_1$ is the width of the laser zone). In this situation expansion compensates for the thermal effect, due to which variation of the gas dynamic parameters with respect to flow is sufficiently smooth in nature. For example, at $r_0 \lesssim 10$ cm, the expansion factor is so significant that essentially no increase of temperature and pressure in the radial direction is observed in the presence of a cavity at $\beta_{He} \approx 10$ and in this case even an appreciable drop of them occurs at the beginning of the zone. At large values of $r_0$ ($r_0$ much greater than $\Delta r_1$), the effect of radial expansion has a low effect within the width of the laser zone. In the given situation the distribution of the gas dynamic parameters essentially coincides with distribution in a flat design. Thus, a sharp temperature and pressure increase begins at $\beta_{He} \approx 10$ even at distances of $\Delta r = r - r_0 \approx 5\text{-}10$ cm, which is accompanied by strong flow retardation (see Figures 2 and 3, the curves for $r_0 = 1$ km). In this case, generation is interrupted usually for a long time until the reagents are used up.

The typical distribution of the total radiation intensity in the active zone is presented in Figure 4. Unlike a HF laser, the main photon scintillation occurs toward the end of the zone in the case of chain excitation in a "cold" reaction. An increase of cylinder radius leads to contraction of the laser zone (see Figures 4 and 5, a).

The geometric factor which affects the gas dynamic and kinetic processes in a radially expanded flow also naturally affects the laser energy parameters. It follows from Figure 5, b that there is an optimum with respect to $r_0$ with fixed degree of fluorine dissociation $\alpha_F$ and degree of dilution $\beta_{He}$. Specifically, the optimum value of the radius comprises $r_0 \approx 15$ cm at

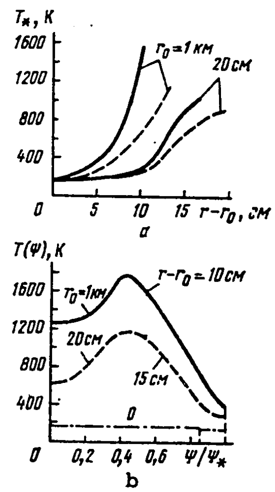


Figure 2. Effect of Design Configuration on Distribution of Mean Temperature of Mixture $T_*$ Along the Flow (a) at $\beta_{He} = 10$ (Solid Curves) and at $\beta_{He} = 15$ (Dashed Curve) and Temperature in Some Cross-Sections (b) at $\beta_{He} = 10$; $p_0 = 15$ mm Hg

$\beta_{He} \approx 10$ and $\alpha_F \approx 15$ percent. The width of the laser zone $\Delta r_1 \approx 20$ cm corresponds to this value of $r_0$ (see Figure 5, a). The specific laser energy comprises $E_0 \approx 1$ kJ/g with an optimum value of $r_0$.

The presence of an optimum with respect to $r_0$ has the following explanation. The flow temperature at the input to the cavity is very low: $T_0 \approx 130$-160K when realizing the chain mechanism of excitation of a continuous HF laser. At these temperatures the chain reaction of hydrogen fluorination initially develops very slowly and, moreover, the diffusion velocity is low during laminar mixing of the streams. At small values of $r_0$, the radial expansion factor compensates for the thermal effect so that the heat released in the reaction is sufficient to heat the mixture to temperatures of approximately 200-300K, at which the reaction accelerates appreciably. The indicated circumstances lead to appreciable extension of the reaction zone and accordingly of the generation zone (see Figure 5, a). The energy parameters of a HF laser decrease with regard to the fact that the rate of deactivation of excited HF molecules (in HF-HF collision processes) is very high at low temperatures [8]. On the other hand, the expansion factor is insignificant at large values of $r_0$. In this situation, interruption of generation, as noted above, occurs long before the reagents are consumed due to the sharp temperature and pressure increase.

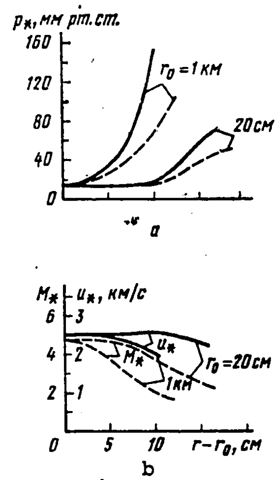


Figure 3. Effect of Design Configuration on Distribution Through Pressure Flow p* (a) at $\beta_{He} = 10$ (Solid Curves), $\beta_{He} = 15$ (Dashed Curve) and Mean Values by the Period of Velocity Values u* and Mach number M* (b) at $\beta_{He} = 10$; $p_0 = 15$ mm Hg

Thus, selection of the optimum nozzle radius plays an important role at fixed values of $\beta_{He}$ and $\alpha_F$. Specific optimization can be accomplished by variation of the degree of dilution at fixed value of $r_0$. It may be noted that the dependence on specific energy $E_0$, the chemical efficiency $\eta_{khim}$ and the given power $P_1$ on $r_0$ is rather sharp in nature at small values of dilution ($\beta_{He} \lesssim 7$-10) and the optimum values of the indicated values decrease with a decrease of $\beta_{He}$. The effect of $r_0$ is much weaker at large values of $\beta_{He}$ ($\gtrsim 15$-20) since the thermal effects are manifested to a lesser degree.

Let us now turn to the results of investigating the dependence of the laser energy parameters on pressure at the nozzle cutoff. It follows from the calculations that the chemical efficiency and specific laser energy essentially do not depend on $p_0$ at pressures of $p_0 \lesssim 10$ mm Hg, while the reduced generation power decreases with a pressure decrease (Figure 6). This means that there is essentially complete mixing of the reagents within the laser zone under these conditions. Further, with laminar nature of mixing the function $P_1(p_0)$, as in the case of a "cold" reaction [4], has an optimum which is explained mainly by the effect of thermal effects on the reagent diffusion rate. Finally, the values of $\eta_{khim}$ and $E_0$ decrease with an increase of pressure at the cutoff (at $p_0 > 10$ mm Hg, which is related to deterioration of the

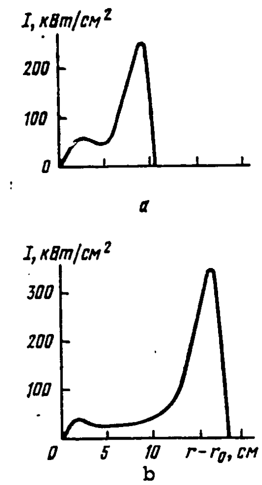


Figure 4. Nature of Total Radiation Density Distribution Along the Laser Zone for Nozzle Radius of $r_0$ = 30 (a) and 15 cm (b) ($p_0$ = 15 mm Hg and $\beta_{He}$ = 10)

mixing conditions, on the one hand, and to reduction of the generation zone on the other hand. Thus, mixing faster than laminar must be provided to operate in the higher pressure zone ($p_0 \approx$ 30-40 mm Hg). A reduction of the width of the laser zone can be compensated in this case by a reduction of the degree of dissociation of $F_2$.

6. Conclusions

Let us formulate the main conclusions ensuing from the given analysis:

1. The configuration of the ring model permits one to realize conditions in the cavity zone for neutralization of the thermal effect and thus to successfully solve the problem of the "thermal" closing of supersonic channels.

2. Very high levels of chemical efficiency (approximately 10 percent) specific laser energy (approximately 1 kJ/g) and corrected laser power (approximately 1 kW/cm$^2$) can be realized with chain excitation at specific operating modes of a ring HF laser.

3. The chain mechanism of excitation permits one to convert to higher static pressures in the cavity zone ($p_0 \approx$ 15-25 mm Hg), which is exceptionally important in solving the ejector problem.

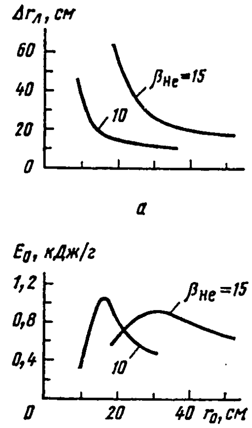


Figure 5. Dependence of Width of Generation Zone (a) and Specific Laser Energy (b) on Nozzle Radius ($p_0$ = 15 mm Hg)

4. Realization of a chain HF laser permits a significant increase of the efficiency of the laser-energy complex as a whole, i.e., the so-called total efficiency of the system [8].

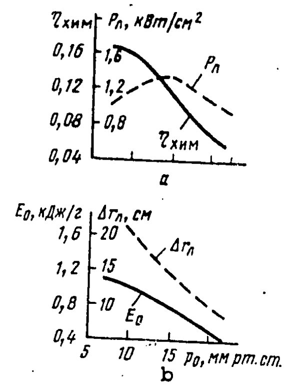

Figure 6. Dependence of Energy Parameters of HF Laser with Chain Excitation on Pressure $p_0$ at the Nozzle Cutoff ($\beta_{He} = 10$ and $r_0 = 20$ cm)

BIBLIOGRAPHY


1. Spencer, D. J., H. Mirels and D. A. Durran, J. APPL. PHYS., Vol 43, 1972.

2. Schulman, E. R., W. G. Burwell and R. A. Meinzer, AIAA Paper No 74-546, 1974.

3. Nagai, C. K., L. W. Carlson, R. R. Giedth and R. D. Klopaten, AIAA Paper No 74-684, 1974.

4. Stepanov, A. A. and V. A. Shcheglov, KVANTOVAYA ELEKTRONIKA, Vol 6, 1979.

5. Finkleman, D. and R. A. Greenberg, AIAA Paper No 75-297, 1975.

6. Warren, W. R., ASTRONAUTICS AND AERONAUTICS, Vol 13, 1975.

7. Orayevskiy, A. N., V. P. Pimenov, A. A. Stepanov and V. A. Shcheglov, KVANTOVAYA ELEKTRONIKA, Vol 3, 1976.

8. Krutova, V. G., A. N. Orayevskiy, A. A. Stepanov and V. A. Shcheglov, KVANTOVAYA ELEKTRONIKA, Vol 3, 1976; ZhTF, Vol 47, 1977.

9. Cummings, J. C. and C. M. Dube, IEEE J., QE-11, 1975; R. A. Meinzer and R. V. Steele, Ibid., 1975.

10. Sadowski, T. J., C. E. Kepler, B. R. Bronfin, M. D. Krosney and R. Roback, Ibid., 1975.

11. Bai, Shih-I, "Vvedeniye v teoriyu techeniya szhimayemoy zhidkosti" [Introduction to the Theory of Flow of a Compressible Liquid], Moscow IL, 1961.

12. Stepanov, A. A. and V. A. Shcheglov, FIAN Preprint, No 182, Moscow, 1976.

13. Dorrens, U. Kh., "Giperzvukovyye techeniya vyazkogo gaza" [Hypersonic Viscous Gas Flows], Moscow, Mir, 1966.

[156-6521]



6521
CSO: 1862

ELECTRICITY AND MAGNETISM

HISTORY AND PROSPECTS FOR TRANSISTOR USE

Moscow PRAVDA in Russian 12 Oct 79 p 3

[Article by Yu. Pozhela, academician of the Lithuanian Academy of Sciences, Lenin Prize Laureat, Vil'nyus: "Wave Melodies of Plasma"]

[Text] It is impossible to think of present-day science and technology or even our everyday life without radio, television, the telephone, computers, lasers, radar and other equipment based on the use of electromagnetic waves. The production of equipment which generates and transforms these oscillations has become the business of whole sectors of industry, radio engineering, communications factilities, electronics and optics. It is precisely these which in many ways determine scientific and technological progress today.

The large-scale changes which have occurred in this area over the past three decades became possible due to the discovery of semiconductor oscillators and generators--transistors. They radically changed the face of radio engineering and led to the formation of new directions for science and technology (microelectronics, high-speed computer technology, etc.).

But transistors are already unable to satisfy the new demands imposed by practice. It has become an urgent requirement that the "busy" signal be eliminated from communication lines; that we learn to transmit energy to the erath from satellite electricpower plants; that we significantly improve the accuracy of aircraft takeoffs and landings and the mooring of ships: that we increase the hgih-speed response of computers. All of these and other problems require the creation of reliable instruments for the so-called superhigh-frequency range which are simple to use.

Transistors are powerless here. Oscillations in the superhigh-frequency range are now transofrmed mainly using complex vacuum devices. However, it is possible to involve other physical phenomena to solve this problem. The plasma effects in semi-conductors may, in our view, serve as this type of phenomenon.

When speaking of plasma, one usually has in mind a "gas" of charged particles which may be displaced, compressed, or stretched using electrical and magnetic fields. Stars, the sun and lightning-discharge paths all consist of plasma. Therefore, the phrase "plasma in semiconductors" at first caused perplexity. However, a more careful examination leads to the conclusion that the "gas" of free electrons and the "vacancy" of positive charges in semiconductors is precisely a plasma, a specific type, it is true, since it is located among atoms which are forming the lattice of a crystal. But nonetheless, it is possible to affect the plasma in a semiconductor with electrical and magnetic fields.

It is known that plasma becomes unstable when an electric current is passed through it: it stretches into a string, it twists into a spiral, it compresses into individual lumps, it starts to undulate. Academician L. Artsemovich said that en route to a controlled thermonuclear reaction "the wave melodies of plasma resound like a funderal march." Similar instabilities are observed in semiconductors. But this only indicates current oscillations, i.e., the generation of electromagnetic waves, the superhigh-frequency range included. Rephrasing Academician L. Artsemovich's words, it is now possible to say that the wave melodies of plasma in semiconductors resound like a triumphal march en route to the creation of superhigh-frequency generators and amplifiers.

In 1959, the Soviet scientist A. Tager and his coworkers detected that during formation of an electron avalanche in silicon, generation of superhigh-frequency oscillations begins. In the following years, research on avalanches and the solution of complex technological problems resulted in the creation of a new class of semiconductor devices--avalanche-transit diodes.

In 1963, the American Physicist George Hann detected generation of superhigh-frequency oscillations when direct current is applied to gallium arsenide.

The Hann diodes and avalanche-transit diodes have today become the basis for inexpensive and reliable instruments of mass application. The wave range in which semiconductors function has been expanded ten-fold. This is a great success for physics and semiconductor technology.

However, in the submillimeter area, instr-ments of this type are also powerless: Their efficiency and the power which is obtainable fall off sharply. Does this perhaps mean that the instabilities in semiconductor plasma have exhausted their possibilities? By no means. In recent years, several ideas have been expressed which permit us tothink that there are more high-frequency instabilities in semiconductor plasma. Thus, S. Ashmontash, K. Repshas and the author of these lines detected that when the electrons in a uniform semiconductor are unevenly heated up, the semiconductor detects superhigh-frequency oscillations well, and generates them itself when direct current is applied. This phenomenon permitted us to create a new type of avalanche diode. Furthermore, the theoretical calculations show that electromagnetic waves in an electric field, heating up plasma electrons, can interact in the region of very high frequencies, leading to the generation and amplification of signals close to the optical range.

Testing these assumptions of the theory requires complex experiments studying the propagation of electromagnetic waves in semiconductors. One must say that superhigh-frequency oscillations in a plasma which conducts electric current well have been generally considered to be impossible for a long time. It was only in 1960 that the Soviet scientists O. Konstantinov and V. Perel' demonstrated that in a magnetic field plasma becomes "transparent" for certain electromagnetic waves, even within a metal.

Now, waves penetrating plasma are being studied in many of the world's laboratories in two respects: on one hand, to study the properties of the semiconductor plasma and, on the other, to reveal the possibilities of generation and amplification of these waves. Such research is being conducted in our country at the Institute of Semiconductor Physics, Academy of Sciences, Lithuanian SSR, the Institute of Radio Engineering and Electronics, Academy of Sciences, USSR and in other Institutes as well as at several VUZ's. New methods for determining the parameters of plasma with the aid of magnetic-plasma waves, and methods for studying high-speed processes in semiconductors have been developed: a millimeter spectroscopy of semiconductors has been born and the activity of plasma in semiconductors applicable to generation and amplification of superhigh-frequencies has been studied.

The results which have been obtained to date instill hope that the mastery of the frequency ranges which have remained until now a blank spot for semiconductor electronics is a matter for the near future. Thus the full scope of the electromagnetic oscillation spectrum will be covered by semiconductor devices, from visible light to the sonic frequencies. It is possible that their creation will permit us to solve the theoretical problems mentioned at the start of the article as well as to open new horizons before the technology of scientific experiment, particularly for the study of these waves on biological subjects.

I will explain that in a given region of the spectrum there are so-called molecular resonances, i.e., frequencies at which molecules interact particularly strongly with waves. It is expected that with the aid of powerful resonance waves, we will succeed in selectively acting on the necessary molecules, and that means that we will actively control various chemical and biological processes. This could enrich the arsenal of measures for controling many illnesses which arise at the molecular level.

As the history of natural science attests, the incorporation of new physical methods and phenomena into practice has always led to revolutionary transformations in science and technology. One would hope that in this case as well, people will receive a powerful instrument for study and for effecting the nature surrounding them into their hands.

Success in solving the problem depends in many ways on the proper organization of research. It should be based on an all-union program of fundamental study of plasma in semiconductors. Development of the program has become an urgent requirements for today, and one must provide experiments in this area with the required materials and equipment.

9194
CSO: 1862

PHYSICS

Crystals and Semiconductors

USSR UDC 548.3:534.01

PHONON DENSITY OF STATES OF SILICON (RESULT OF SOLUTION OF THE INVERSE PROBLEM)

Tomsk FONONNAYA PLOTNOST' SOSTOYANIY KREMNIYA (REZUL'TAT RESHENIYA OBRATNOY ZADACHI) in Russian, editorial board of "Izvestiya VUZov, Fizika," 1979 6 pp (manuscript deposited in VINITI 23 Jan 79, No 309-79 Dep.)

KORSHUNOV, V. A.

[From REFERATIVNYY ZHURNAL, FIZIKA No 4, 1979 Abstract No 4Ye259 DEP by the author]

[Text] The inverse problem of the determination of the density of states from the temperature dependence of the heat capacity of phonons belongs to the class of incorrectly posed problems. It is solved by the method of regularization with a Tikhonov stabilizer of first order. The regularization parameter is selected by the principle of minimum error of closure which, as is shown by the example presented for a silicon crystal, permits the determination of the characteristic structure of the phonon density of states in satisfactory correspondence with existing neutron diffraction data. References 21.

[11,574-147]

USSR UDC 548.536

STRUCTURE AND THERMOPHYSICAL CHARACTERISTICS OF THE COMPOUND $Mg_2Hf_5O_{12}$

Tomsk STRUKTURNYYE I TEPLOFIZICHESKIYE KHARAKTERISTIKI SOYEDINENIYA $Mg_2Hf_5O_{12}$ in Russian, editorial board of "Izvestiya VUZov, Fizika," 1979, 10 pp (manuscript deposited in VINITI 2 Jan 79, No 18-79 Dep.)

MALETS, YE. B. and ZOZ, YE. I.

[From REFERATIVNYY ZHURNAL, FIZIKA 1979 No 4, Abstract No 4Ye313 DEP by the author]

[Text] Results of research on composition of the system $HfO_2$-$MgO$, containing 20-30 mol.% of MgO are given. It is shown that this system contains the compound $Mg_2Hf_5O_{12}$ crystalized in a rhombohedral distorted lattice of the fluorite type. $Hf_3Yb_4O_{12}$, $Zr_3Yb_4O_{12}$ and $Zr_3Sc_4O_{12}$ are crystallographic analogies of this compound. The temperature and concentration dependence of the specific conductivity of the above mentioned compositions were obtained. The activation energy of the process responsible for conductivity was $0.6 \pm 0.1$ eV. Data on the concentration and mobility of vacancies in the compositions studied are given. The coefficient of linear thermal expansion of $Mg_2Hf_5O_{12}$ is $\alpha = 4.63 \cdot 10^{-6}$ °C. The melting point is above 2300°C. References 11.

[11,574-147]

USSR UDC 548:539

INVESTIGATION OF LOW-TEMPERATURE AGE IN Cu-Al -SOLID SOLUTIONS SUBJECTED TO PLASTIC DEFORMATION AT -196°C

Tomsk IZUCHENIYE NIZKOTEMPERATURNOGO VOZRASTA V α-TVERDYKH RASTVORAKH Cu-Al, PLASTICHESKI DEFORMIROVANNYKH PRI -196°C in Russian, editorial board of "Izvestiya VUZov, Fizika," 1979, 10 pp

ZUBCHENKO, V. S., KULISH, N. P. and PETRENKO, P. V.

[From REFERATIVNYY ZHURNAL, FIZIKA No 4, 1979 Abstract No 4Ye417DEP by the authors]

[Text] Two stages corresponding to the second and third age stages of pure copper are determined from the age curves of specific conductivity of Cu-Al alloys (6, 8, 10, 13, 15 and 17 at.% Al) and pure copper, subjected to plastic deformation in liquid nitrogen. The change in conductivity on the second stage is due to drift of defects that are ineffective in formation of short-range order, and the conductivity change on the third stage is due to vacancy drift, and to an increase in the degree of short-range order as a result of such migrations. It is concluded from the concentration dependence of the conductivity increment on the third stage that consideration must be taken of the influence of defects introduced during deformation when comparing the theoretical and experimental values of conductivity of deformed specimens. References 8.

[11,574/6610-147]

USSR UDC 536.421

CALCULATING THE RATE OF GROWTH OF CRYSTALS FROM A TWO-COMPONENT MELT IN A CENTRIFUGAL FIELD

Moscow RASCHET SKOROSTI ROSTA KRISTALLOV, RASTUSHCHIKH IZ DVUKHKOMPONENTNOGO RASPLAVA V TSENTROBEZHNOM POLE in Russian, editorial board of "Vestnik Moskovskogo gosudarstvennogo universiteta, Khimiya," 1978, 10 pp (manuscript deposited in VINITI 23 Nov 78, No 3576-78 Dep.)

ANIKIN, A. G. and TAL'DRIK, A. F.

[From REFERATIVNYY ZHURNAL, FIZIKA No 4, 1979 Abstract No 4Ye458DEP by the authors]

[Text] A theoretical examination is made of the problem of the behavior of the growth rate of two-component crystals when grown from a melt in a centrifugal force field. A system of nonlinear equations of the thermal and diffusion layers is derived with consideration of the influence that the growth rate of the crystal phase has on interrelated heat and mass processes. Relations are found for the thickness of boundary layers and for crystal growth rate as functions of the magnitude of the centrifugal field, the coefficients of viscosity and thermal conductivity, dopant diffusion, azimuthal angle, heat of crystallization, specific heat, density of the solid and liquid phases, and the cryoscopic constant. It is shown that crystal growth is asymmetric. See also Ref. zh. Fizika, Abstract No 2Ye415. References 10.

[11,574/6610-247]

USSR UDC 537.226;537.311.322

OPTICAL PROPERTIES OF $RbAg_4I_5$ SUPERIONIC THIN-FILM CONDUCTORS

Tomsk OPTICHESKIYE SVOYSTVA TONKIKH PLENOK SUPERIONNOGO PROVODNIKA $RbAg_4J_5$ in Russian, editorial board of "Izvestiya VUZov, Fizika," 1979, 10 pp (manuscript deposited in VINITI 2 Jan 79, No 33-79 Dep.)

DROZDOV, V. A., MALASHCHENKO, T. V. and MURAKHOVSKIY, V. G.

[From REFERATIVNYY ZHURNAL, FIZIKA No 4, 1979 Abstract No 4Ye 1105DEP (resume)]

[Text] The reflection and absorption spectra of $RbAg_4I_5$ superionic thin-film conductors are studied as a function of temperature. Thermal coefficients are calculated for the absorption edge and for the reflection maximum associated with quasimetallic silver centers. Kramers-Kronig dispersion relations are used to calculate the coefficients of absorption and refraction, and the real and imaginary parts of the dielectric constant. It is suggested on the basis of the calculation that the valence band of $RbAg_4I_5$ is formed by Ag(4d)- and I(5s)-states, while the conduction band is formed by the Rb(4d) and Ag(5s) states. References 7.

[11,574/6610-247]

USSR UDC 537.226.4

TRANSITIONS BETWEEN FERROELECTRIC PHASES IN OXIDE SOLID SOLUTIONS WITH PEROVSKITE STRUCTURE

Tomsk PEREKHODY MEZHDU SEGNETOELEKTRICHESKIMI FAZAMI V TVERDYKH RASTVORAKH OKISLOV SO STRUKTUROY TIPA PEROVSKITA in Russian, editorial board of "Izvestiya VUZov, Fizika," 1979, 9 pp (manuscript deposited in VINITI 2 Jan 79, No 16-79 Dep.)

RAYEVSKIY, I. P. and SYTOVA, O. N.

[From REFERATIVNYY ZHURNAL, FIZIKA No 4, 1979 Abstract No 4Ye1265DEP by the authors]

[Text] It is experimentally shown that the experimental rule of Bretton and T'yen for predicting the change in temperatures of transitions between ferroelectric phases in $BaTiO_3$ with ion substitutions in one of the cationic sublattices is applicable to $KNbO_3$ as well. A modification of this rule is proposed for the case where ion substitution takes place simultaneously in both cationic sublattices. The described rule is also applicable in the case of systems of solid solutions that are more complicated than binary solutions. References 11.

[11,574/6610-247]

USSR

UDC 537.226.4

ON LOCALIZATION OF RARE EARTH CATIONS IN THE BARIUM TITANATE LATTICE

Tomsk O LOKALIZATSII REDKOZEMEL'NYKH KATIONOV V RESHETKE TITANATA BARIYA in Russian, editorial board of "Izvestiya VUZov, Fizika," 1979, 6 pp (manuscript deposited in VINITI 2 Jan 79, No 20-79 Dep.)

DERGUNOVA, N. V., SAKHNENKO, V. P. and FESENKO, YE. G.

[From REFERATIVNYY ZHURNAL, FIZIKA No 4, 1979 Abstract No 4Ye1283DEP by the authors]

[Text] Interpretation of the peculiarities of concentration dependences of conductivity of semiconductor modifications of $BaTiO_3$ requires solution of the general problem of localization of extrinsic ions in the crystal lattice with perovskite structure. This problem is solved within the framework of a quasielastic crystal model for low concentrations of extrinsic ions (less than 0.1 at .%). It is shown that in this concentration region, rare earth extrinsic ions from La to Tm primarily replace titanium cations, while Yb and Lu primarily replace barium cations. At concentrations higher than 0.1 at .%, cations from La to Tm are localized mainly in sublattice A, while Yb and Lu are localized in sublattice B, according to the conventional rules of isomorphism. A transition from B-substitution to A-substitution should be accompanied by a sharp drop in resistivity in the vicinity of concentrations near 0.1%, which agrees with the experimental data. References 7.

[11,574/6610-247]

USSR

UDC 537.611.44

PROCESSES OF INTRAPHASE SEGREGATION IN Fe-V ALLOYS

Moscow PROTSESSY VNUTRIFAZNOY SEGREGATSII V SPLAVAKH Fe-V in Russian, Moscow State University, 1978, 16 pp (manuscript deposited in VINITI 7 Feb 79, No 251-79 Dep.)

STETSENKO, P. N. and ANTIPOV, S. D.

[From REFERATIVNYY ZHURNAL, FIZIKA No 4, 1979 Abstract No 4Ye1346DEP by the authors]

[Text] The process of dissociation of an iron-vanadium alloy (45 at.% Fe and 55% V) after quenching from 1350°C is studied by the methods of

Mössbauer spectroscopy on $^{57}Fe$ nuclei and the temperature dependence of the intensity of magnetization. The results show that heat treatment up to 625°C leads to processes of intraphase segregation with retention of the single-phase nature of the specimen. As a result of these processes, the alloy contains iron-rich and iron-poor magnetic clusters with characteristics that vary depending on heat treatment. Since the observed processes of intraphase segregation are characterized by low activation energies, the authors discuss the vacancy mechanism of cluster formation. References 10.

[11,574/6610-247]

USSR UDC 532.783;548-14

CONDUCTIVITY OF A p-AZOXYANISOLE LIQUID CRYSTAL

Tomsk PROVODIMOST' ZHIDKOGO KRISTALLA p-AZOKSIANIZOLA in Russian, editorial board of "Izvestiya VUZov, Fizika," 1979, 10 pp (manuscript deposited in VINITI 2 Jan 79, No 26-79 Dep.)

NIKITIN, YE. N.

[From REFERATIVNYY ZHURNAL, FIZIKA No 4, 1979 Abstract No 4I236DEP by the author]

[Text] The conductivity of a nematic liquid crystal of p-azoxyanisole is measured, using direct current and low-frequency alternating current. Consideration is taken of individual factors that influence conductivity: temperature, voltage and frequency. The measurements show that domains made up of about $10^5$ molecules move in the wake of an audio frequency field, rather than isolated molecular dipoles. References 5.

[11,574/6610-247]

Electricity and Magnetism

USSR UDC 548:539

STRAIN DEPENDENCE OF PHOTOSTIMULATED EXOELECTRONIC EMISSION OF POLYCRYSTALLINE ALUMINUM

Tomsk ZAVISIMOST' FOTOSTIMULIROVANNOY EKZOELEKTRONNOY EMISSII POLIKRISTALLICHESKOGO ALYUMINIYA OT VELICHINY DEFORMATSII in Russian, editorial board of "Izvestiya VUZov, Fizika," 1979, 8 pp (manuscript deposited in VINITI 23 Jan 79, No 300-79 Dep.)

PARTSYRNYY, V. D. and SOLOSHENKO, I. I.

[From REFERATIVNYY ZHURNAL, FIZIKA No 4, 1979 Abstract No 4Ye386DEP by the authors]

[Text] A relation between the current density of photostimulated exoelectronic emission and strain is found, based on the assumption that the change in work function of metallic emitters as a result of plastic deformation is initially caused by a change in the dislocation density. The strain dependence of current density of photostimulated exoelectronic emission o polycrystalline aluminum as measured during deformation agrees qualitatively with the calculated dependence in the case where stimulation occurs in the subthreshold frequency region. References 13.

[11,574/6610-147]

USSR UDC 537.226; 537.311.322

OPTICAL PROPERTIES OF THIN FILM SUPERION CONDUCTOR $RbAg_4J_5$

Tomsk IZV. BUZOV. SER. FIZIKA in Russian 1979 10 pp

DROZDOV, V. A., MALASHCHENKO, T. V. and MURAKHOVSKIY, V. G.

[From REFERATIVNYY ZHURNAL, FIZIKA No 4 (II) 1979 Abstract No 4E1105 DEP by the author]

[Text] A study of the temperature dependence of the emission and reflection spectra of thin film superion conductor $RbAg_4J_5$. The thermal coefficient of the boundary of absorption and the maximum reflection when bound with quasimetallic centers of silver are calculated. Using the Kramers - Kroning dispersion ratio, the coefficients of absorption and reflection, the actual and imaginary parts of the dielectric and the permeability are calculated. On the basis of the computations it is assumed that the valence bands of $RbAg_4J_5$ are formed by Ag(4d) and J(5s) states and the conduction band by the Rb(4d) and Ag(5s) states. Abstract, illustrations, references 7.

USSR UDC 537.226.4

TRANSITIONS BETWEEN FERROELECTRIC PHASES IN SOLID SUSPENSIONS OF IOXIDES WITH PEROVSKITE TYPE STRUCTURES

Tomsk IZV. VUZOV. SER. FIZIKA in Russian 1979 9 pp

RAYEVSKIY, I. P. and SYTOVA, O. N.

[From REFERATIVNYY ZHURNAL, FIZIKA No 4 (II) 1979 Abstract No 4E1265 DEP by author]

[Text] It is experimentally established that the empirical rule of Bretton and T'yen, permitting the prediction of the character of the changes of the temperature transitions between ferroelectric phases in $BaTiO_3$ in cases of ion replacement in one of the ion sublattices is also applicable to $KNbO_3$. A modification of this rule is suggested for cases where ion replacement is simultaneous in both ion sublattices. The rule described is also applicable in cases of solid suspension systems which are more complicated than binary ones. Illustrations, references 10.

USSR UDC 537.611.44

ANOMALIES IN THE TEMPERATURE DEPENDENCE OF MAGNETIZATION OF Fe-V ALLOYS

Moscow ANOMALII TEMPERATURNOY ZAVISIMOSTI NAMAGNICHENNOSTI SPLAVOV Fe-V in Russian, Moscow State University, 1978, 15 pp (manuscript deposited in VINITI 7 Feb 79, No 522-79 Dep.)

STETSENKO, P. N. and ANTIPOV, S. D.

[From REFERATIVNYY ZHURNAL, FIZIKA, No 4, 1979 Abstract No 4Ye1347DEP by the authors]

[Text] The paper gives the results of experimental studies of nuclear gamma resonance spectra on $^{57}Fe$ nuclei in Fe-V alloys (45 at.% Fe and 55 at.% V). The temperature behavior of magnetization of Fe-V alloy quenched from 1350°C shows a number of anomalies that the authors attribute to magnetic transitions in intraphase segregations. Data on hyperfine magnetic fields on $^{57}Fe$ nuclei confirm the results of the magnetic measurements. Estimates are made of the critical concentrations at which the exchange integral that characterizes an interaction of the Fe-V type becomes negative. After a number of heat treatments, an equiatomic alloy of iron and vanadium shows a magnetic anomaly analogous to the magnetic compensation point in ferromagnetics. References 11.

[11,574/6610-247]

USSR UDC 537.611.44

INHOMOGENEITY OF MAGNETIZATION OF FINE PARTICLES OF $CrO_2$

Moscow NEODNORODNOST' NAMAGNICHENNOSTI MELKIKH CHASTITS $CrO_2$ in Russian, Moscow State University, 1978, 11 pp (manuscript deposited in VINITI 10 Jan 79, No 93-79 Dep.)

SHPIN'KOV, N. I. and OLEFIRENKO, P. P.

[From REFERATIVNYY ZHURNAL, FIZIKA No 4, 1979 Abstract No 4Ye1351DEP]

[Text] The coercive force, the distribution functions for particles by fields of magnetic reversal and by orientations, and the parameters of ferromagnetic resonance spectra in the frequency range of 36-61 GHz at temperatures of 100-420 K are determined for an ensemble of $CrO_2$ particles.

It is shown that particles with a ratio of length to diameter that exceeds a certain critical value are magnetically inhomogeneous. The way that the shape of the ferromagnetic resonance line depends on temperature and frequency indicates a reduction in the degree of magnetic inhomogeneity as the intensity of magnetization decreases and the external magnetic field increases. It is assumed that the reason for this is a magnetic structure of helicoid type that arises in "transcritical" particles, and that has a wavelength that increases with a reduction in the ratio of magnetization intensity to external field strength. References 6.

[11,574/6610-247]

USSR UDC 537.621

MEASUREMENT OF THE INTENSITY OF MAGNETIZATION IN PULSED MAGNETIC FIELDS OF UP TO 240 MA/m OVER A WIDE RANGE OF TEMPERATURES AND PRESSURES

Minsk IZMERENIYE NAMAGNICHENNOSTI V IMPUL'SNYKH MAGNITNYKH POLYAKH DO 300 ke V SHIROKOM DIAPAZONE TEMPERATUR I DAVLENIY in Russian, Izvestiya Akademii nauk BSSR, Seriya fiziko-tekhnicheskikh nauk, 1979, 14 pp (manuscript deposited in VINITI 11 Jan 79, No 117-79 Dep.)

DOBRYANSKIY, V. M.

[From REFERATIVNYY ZHURNAL, FIZIKA No 4, 1979 Abstract No 4Ye1302DEP]

[Text] A facility has been developed for measuring the intensity of magnetization over a wide range of pressures, temperatures and pulsed magnetic fields. The design of the solenoid located in the high-pressure chamber is described. A description is given of the measurement instrumentation, and automatic equipment for holding the temperature in a range of 4.2-400 K. The paper describes the technique used in the service entrance for supplying the voltage to the solenoid at up to 3000 V in a high-pressure chamber where the gas transmits a pressure of up to $1.5 \cdot 10^9$ N/m$^2$. An investigation is made of the uniformity of the magnetic field. References 14.

[11,574/6610-247]

USSR UDC 537.533.3;537.534.3

AN IMPROVED UNIVERSAL ELECTRON-ION SOURCE

Tomsk USOVERSHENSTVOVANNYY UNIVERSAL'NYY ELEKTRONNO-IONNYY ISTOCHNIK in Russian, Tomsk Polytechnical Institute, 1978, 11 pp (manuscript deposited in VINITI 23 Jan 79, No 276-78 Dep.)

GAVRILOV, N. V., PONOMAREV, V. P. and PONOMAREVA, L. P.

[From REFERATIVNYY ZHURNAL, FIZIKA No 4, 1979 Abstract No 4Zh472DEP by the authors]

[Text] The paper describes a universal electron-ion source based on a reflex discharge with cold cathodes. The source is designed for operation as the injector for an EG-2.5 electrostatic generator. The source provides 10 mA of ion current and 3 mA of electron current with discharge power of no more than 40 W, emission aperture of 0.9 mm and extracting voltage of 10 kV. An investigation is made of the mass composition of the beam under various working conditions. Hydrogen is used as the working gas. Gas flowrate is 20 cc/hr. References 6.

[11,574/6610-247]

Theoretical Physics

USSR UDC 537.8.029.6

ON THE J-PROPERTIES OF THE TRANSFER MATRIX OF A WAVEGUIDE WITH A LOCALIZED IRREGULARITY

Khar'kov O J-SVOYSTVAKH PEREDATOCHNOY MATRITSY VOLNOVODA S LOKALIZOVANNOY NEREGULYARNOST'YU in Russian, Khar'Kov University, 1978, 11 pp (manuscript deposited in VINITI 2 Jan 79, No 48-79 Dep.)

EL'KIN, B. S.

[From REFERATIVNYY ZHURNAL, FIZIKA No 4, 1979 Abstract No 4Zh309DEP]

[Text] An examination is made of the problem of transmission of electromagnetic waves in waveguides with a localized irregularity and two sets of associated problems. It is shown that the transfer matrices ($S_{RN}$, $S_{AN}$, N = 1, 2...) of these problems are expressed in terms of blocks of the transfer matrix (S) of the transmission problem. References 5.

[11,574/6610-247]

Thermodynamics

USSR UDC 530.161/.162

AN ENTROPY CRITERION OF STABILITY

Tomsk ENTROPIYNYY KRITERIY USTOYCHIVOSTI in Russian, editorial board of "Izvestiya VUZov, Fizika," 1979, 9 pp (manuscript deposited in VINITI 2 Jan 79, No 24-79 Dep.)

PEREVOZNIKOV, YE. N. and MASLOV, P. G.

[From REFERATIVNYY ZHURNAL, FIZIKA No 4, 1979 Abstract No 4I23DEP by the authors]

[Text] A general stability criterion is constructed on the basis of the definition of entropy. An examination is made of forms of the criterion in the case of the canonical and projection methods of description. It is shown how the entropy criterion is related to the Glensdorf-Prigogine theory, the spectral method and the Rayleigh criterion. Formulas are proposed for the macroscopic probability of fluctuations in the unstable and metastable states that are transformed to the known Einstein and Glensdorf-Prigogine relations in the case of equilibrium and quasi-equilibrium states. References 10.

[11,574/6610-247]

USSR UDC 548.571

INVESTIGATION OF THE INFLUENCE THAT HELIUM INTRUSION HAS ON THE PHYSICO-CHEMICAL PROPERTIES OF A SOLID

Vladivostok IZUCHENIYE VLIYANIYA VNEDRENIYA GELIYA NA FIZIKO-KHIMICHESKIYE SVOYSTVA TVERDOGO TELA in Russian, 1978, 81 pp (manuscript deposited in VINITI 25 Dec 78, No 3904-78 Dep.)

KHUDYAKOV, A. V.

[From REFERATIVNYY ZHURNAL, FIZIKA No 4, 1979 Abstract No 4Ye323DEP by the author]

[Text] Known and original data are systematized on the properties of defects produced by helium atoms and vacancies in a crystal lattice. A table of properties is compiled, some properties of the table are analyzed, and a prediction is made on the feasibility of a directed change in fundamental properties of a crystal by changing the concentration of certain kinds of defects. Experimental data are given on an increase by 6-8 orders of magnitude in processes controlled by surface diffusion in materials with interstitial helium concentration of $10^{19}$ $cm^{-3}$ and accumulated vacancy concentrations of $2 \cdot 10^{21}$ $cm^{-3}$. This effect has been used to produce beryllium oxide specimens with grain size of less than 1 μm that are resistant to reactor irradiation. An analysis is made of the possibility of a reduction in cohesive energy of a crystal with an increase in the concentration of helium atoms in the lattice site substitution state. The paper gives the approximate behavior of cohesive energy, critical temperatures and pressures of phase transitions as a function of helium concentration in the crystal. A reduction of the cohesive energy of a crystal can be used to reduce the work function of electrons and ions, to create a high concentration of defects of exciton type in covalent crystals, to get metastable phase states (amorphous metals, high-temperature and high-pressure phases) at reduced temperatures and pressures, and to produce superporous solids. References 28.

[11,574/6610-147]

CSO: 1862 - END -



APPROVED FOR RELEASE: 2007/02/08: CIA-RDP82-00850R000200020028-7